Study of Cosmic Ray Anisotropy

Wei Liu

Collaborators: Hong-bo Hu, Yi-qing Guo, Chao Jin, Xiao-chuan Chang, Xiao-bo Qu

2017 LHAASO workshop, Wei Hai

Outline

- Measurements of Galactic cosmic ray anisotropy
- Possible origin of dipole anisotropy
- Large-scale regular magnetic field
- Cosmic ray anisotropic diffusion
- Results
- Summary

Measurements of Galactic cosmic ray anisotropy

Subject to the frequent scattering by the turbulent magnetic field, the arrival directions of Galactic cosmic rays are highly isotropic.

Nevertheless, observations still find the weak anisotropy of arrival distributions, with relative intensities roughly 10^{-3}.

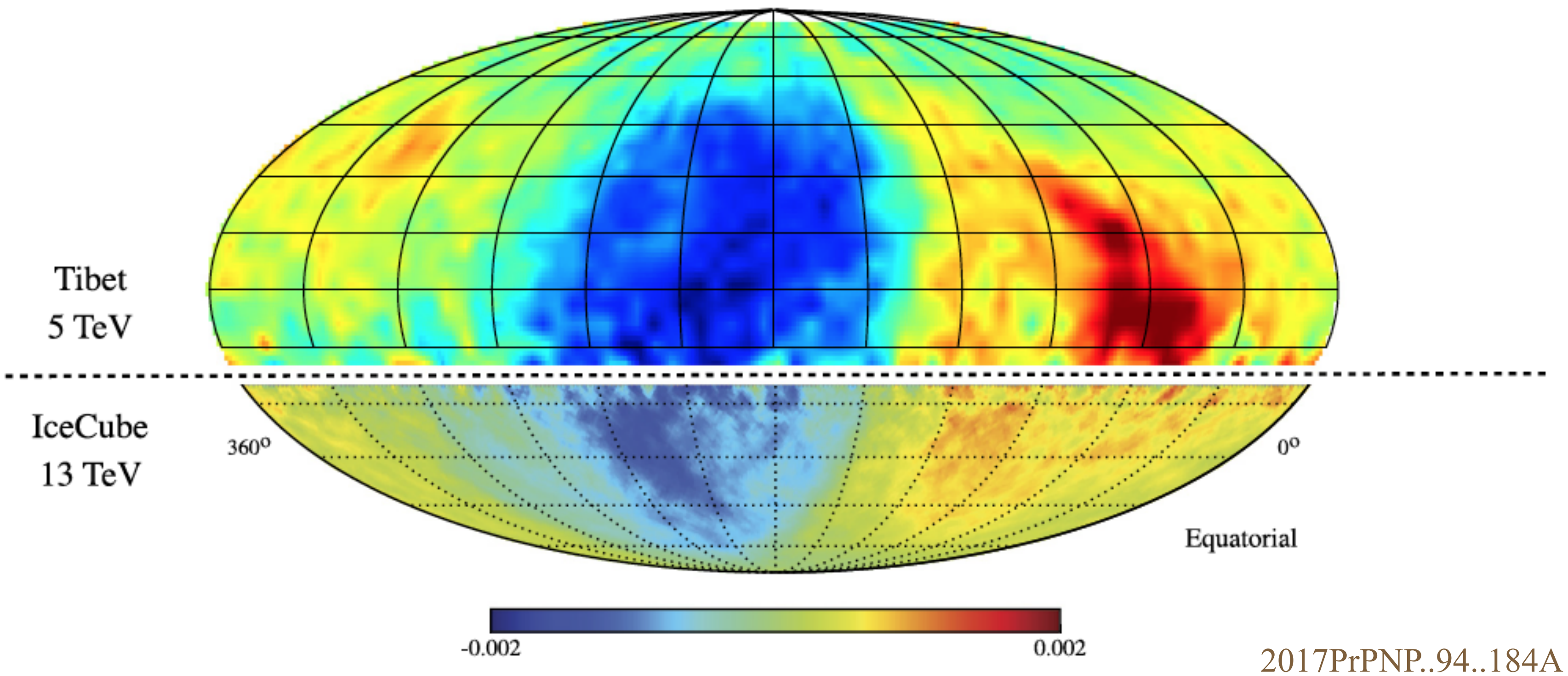

2017PrPNP..94..184A

Combined cosmic ray anisotropy of Tibet-ASgamma and IceCube

On large scale, there are three major regions,

I ———Tail-in,

II ———Loss-cone,

III———Cygnus region

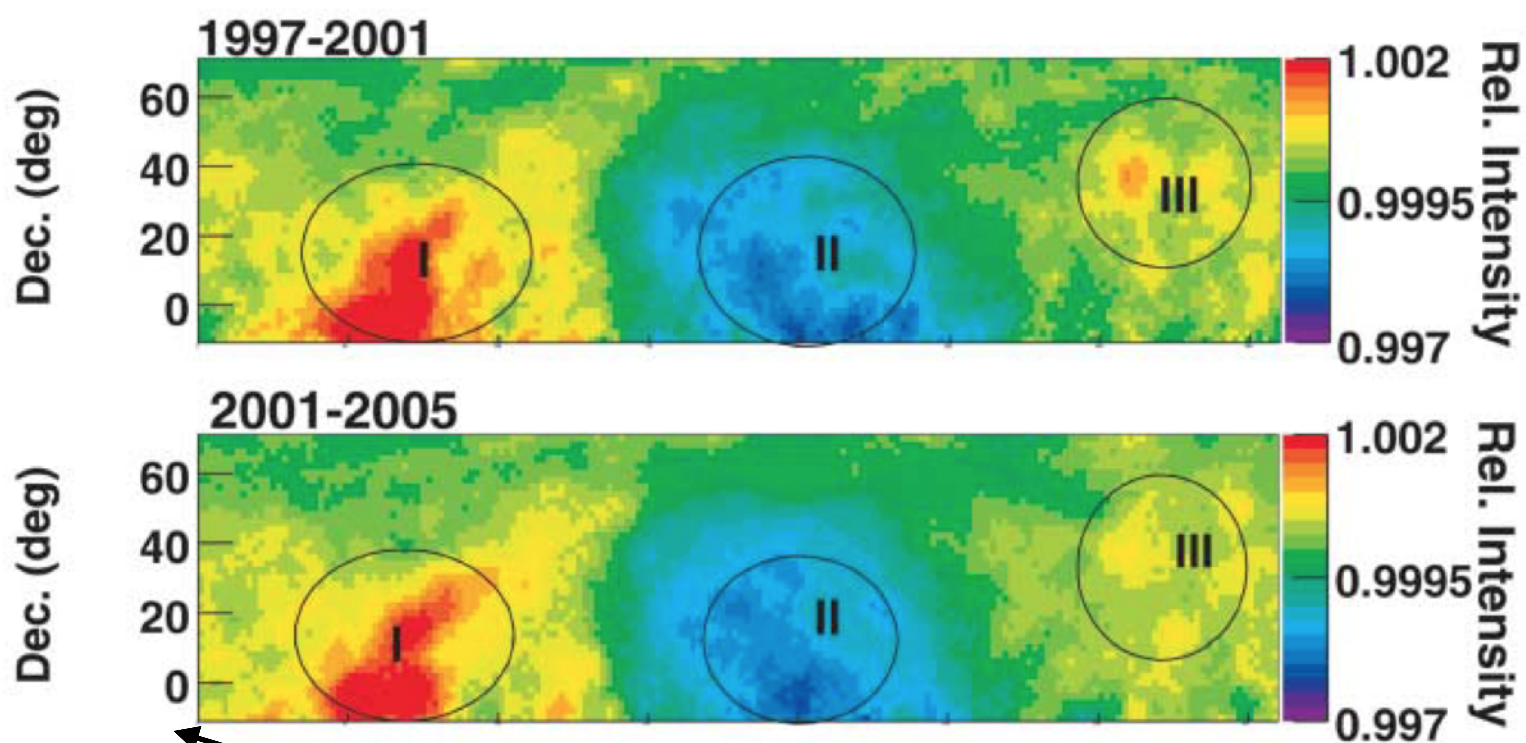

Sidereal time Anisotropy in two hemisphere

M. Amenomori, 2006Sci...314..439A

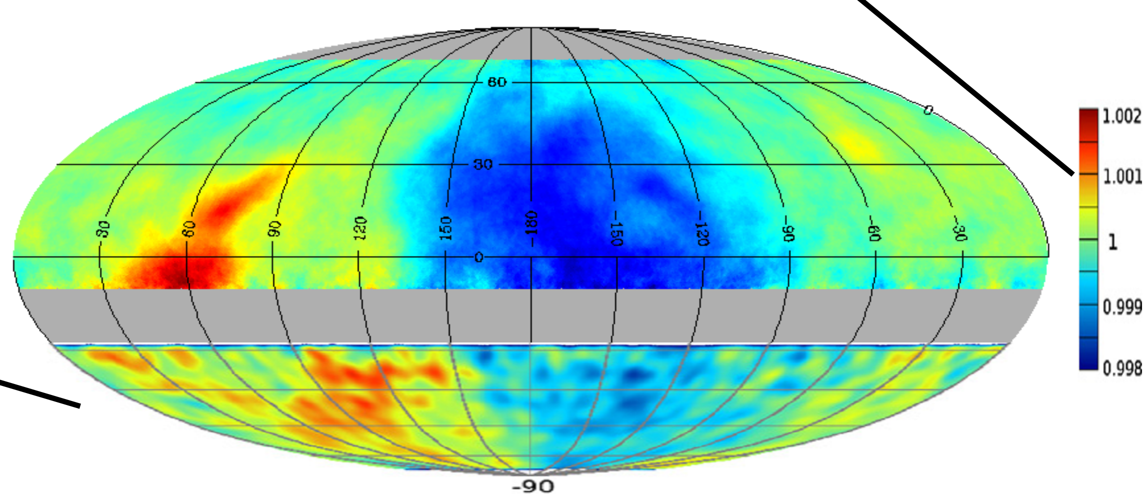

Sidereal time Anisotropy in Galactic coordinate

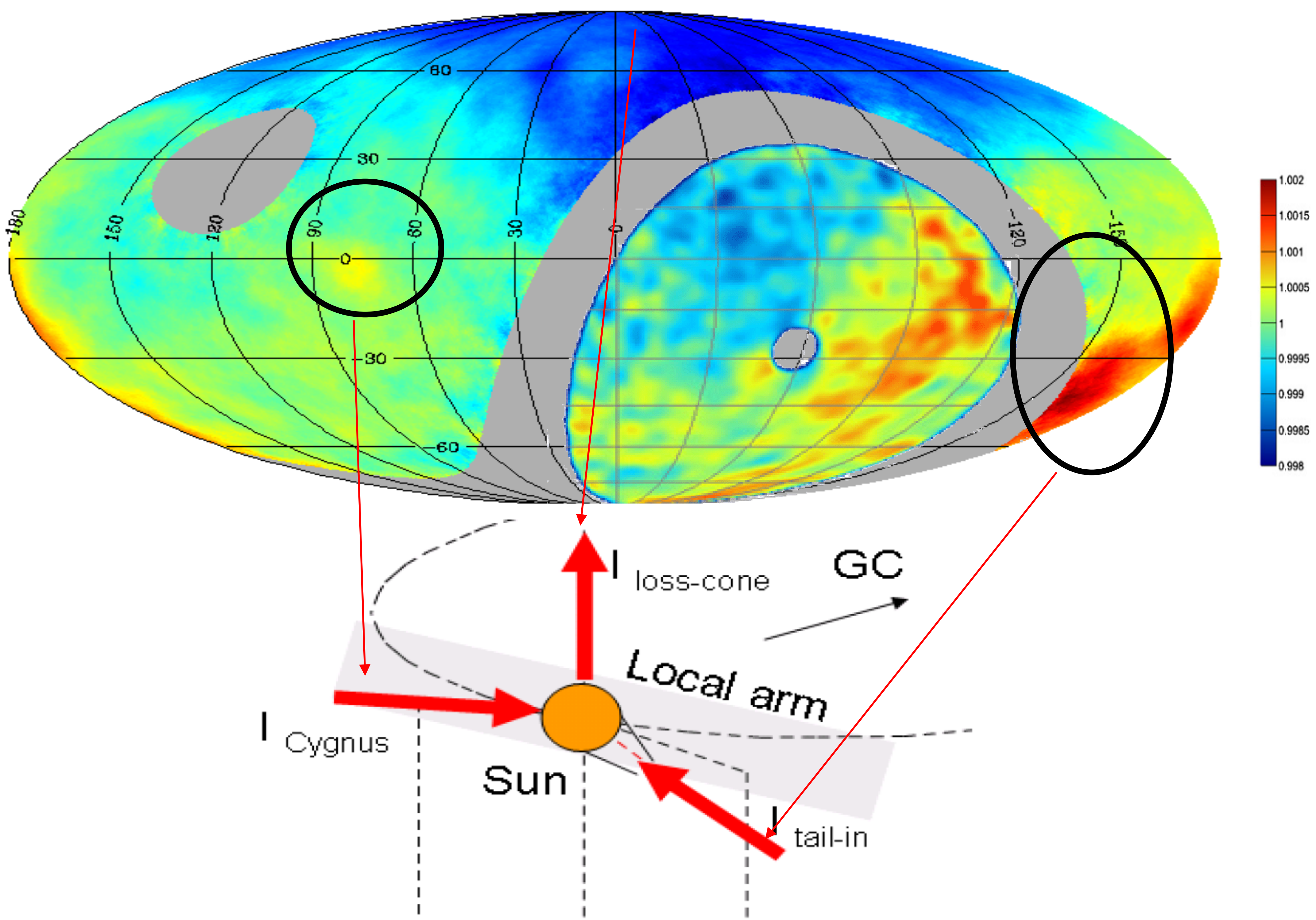

Energy dependence

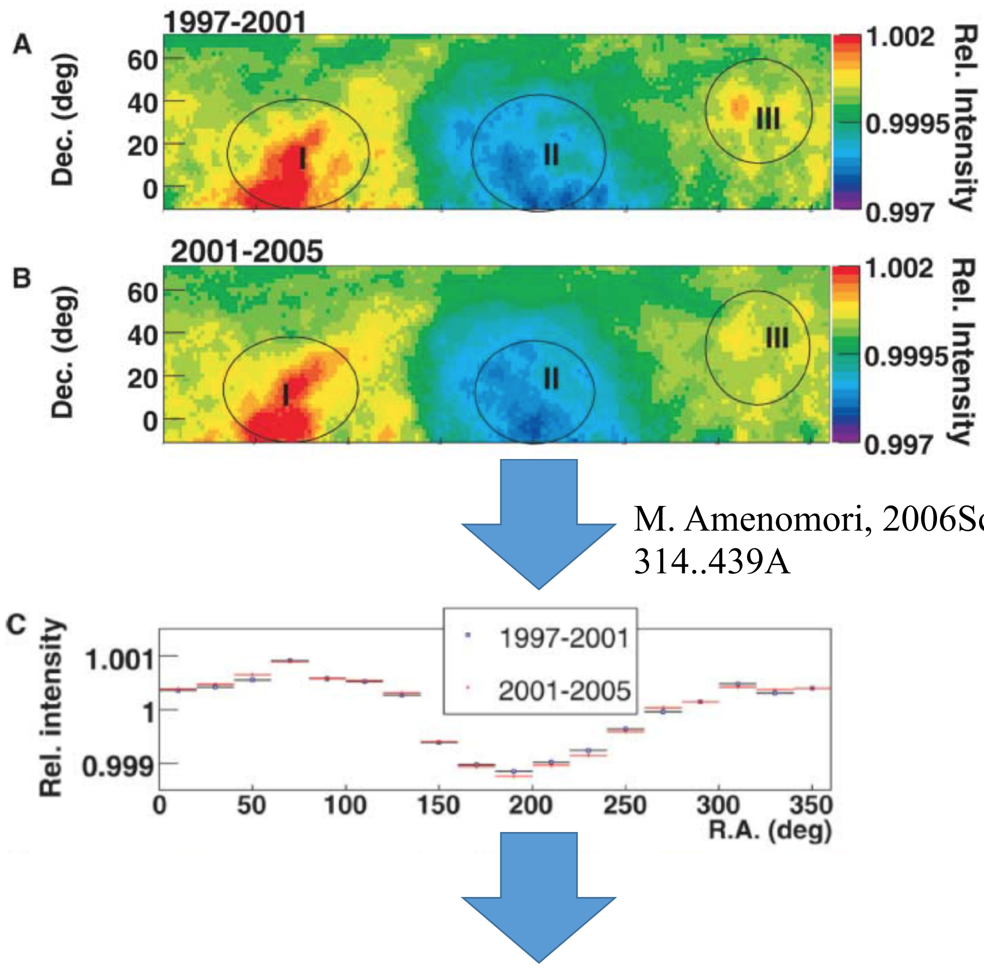

M. Amenomori, 2006Sci... 314..439A

$$R(\alpha) = 1 + A_1 \cos(\alpha - \phi_1)$$

$R(\alpha)$: the relative intensity of CRs at R.A.

2D anisotropy

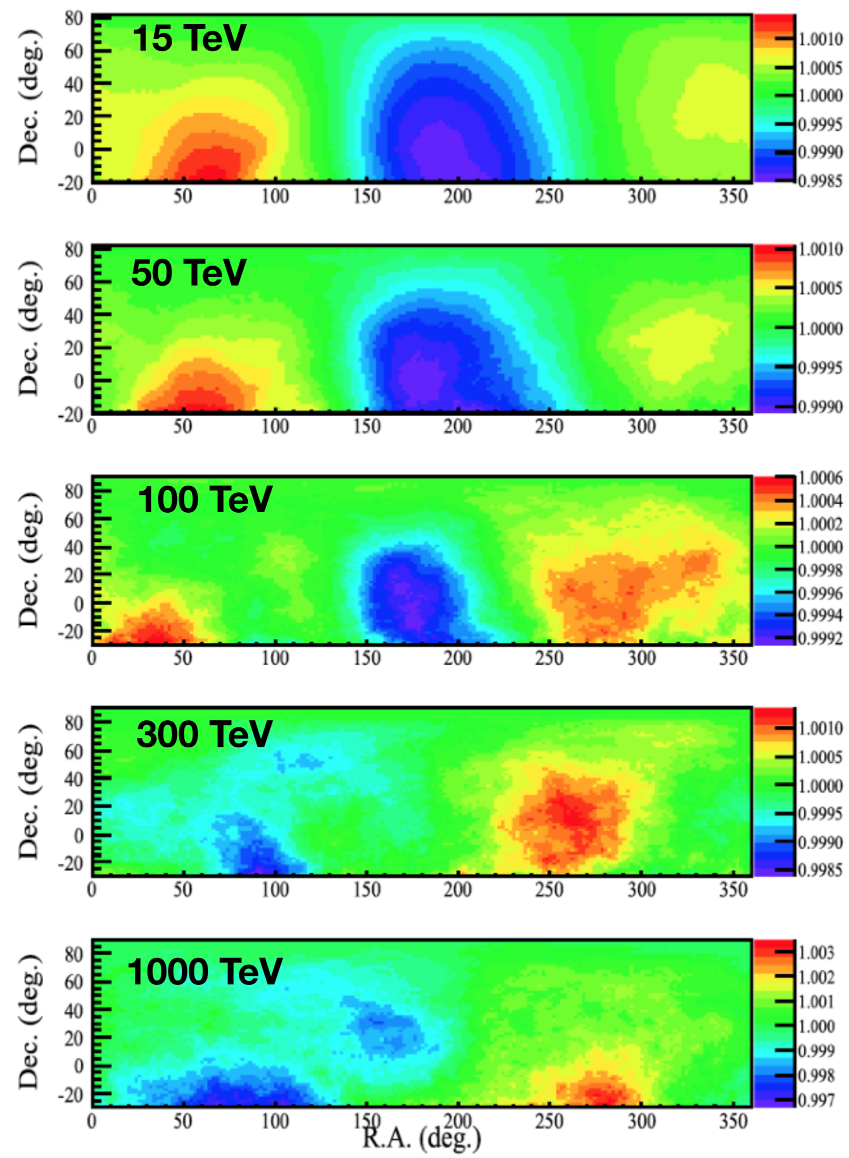

1D projections

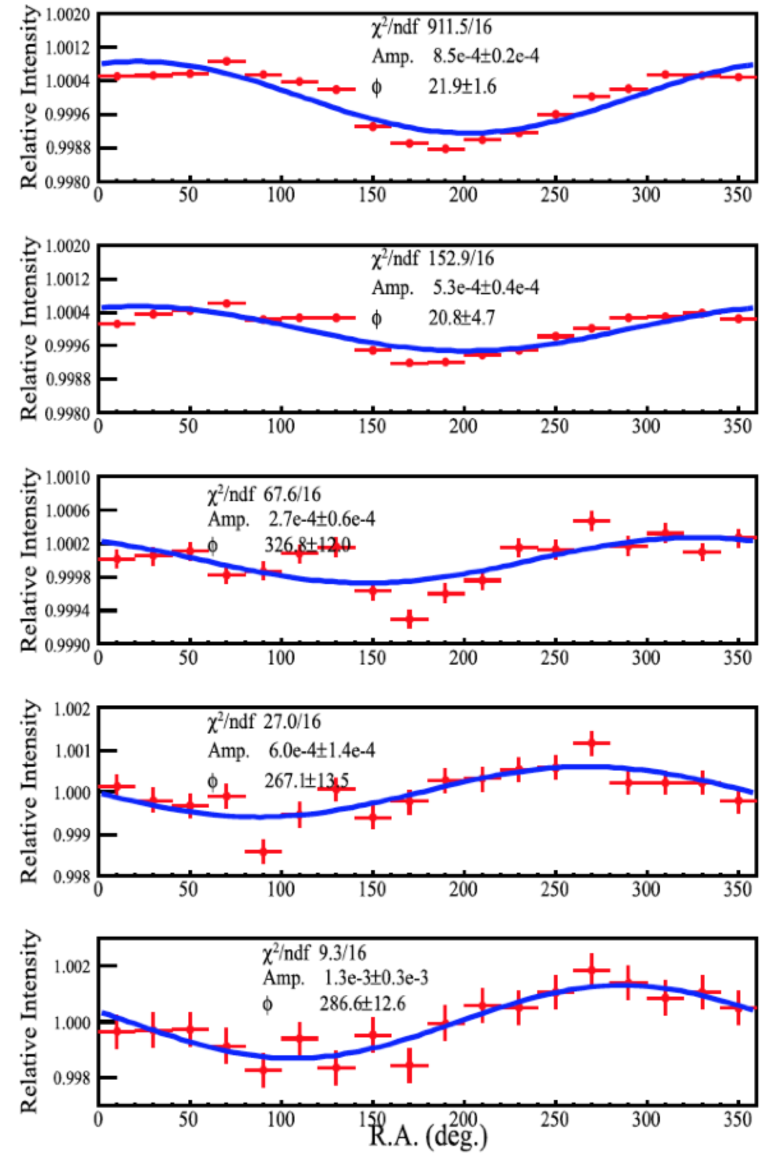

M. Amenomori, 2017ApJ…836..153A

Energy dependence of 2D anisotropy

ARGO-YBJ

- data from 2008
- 365 days livetime
- $6.5 \cdot 10^{10}$ events
- median CR energy ~ 1.1 TeV

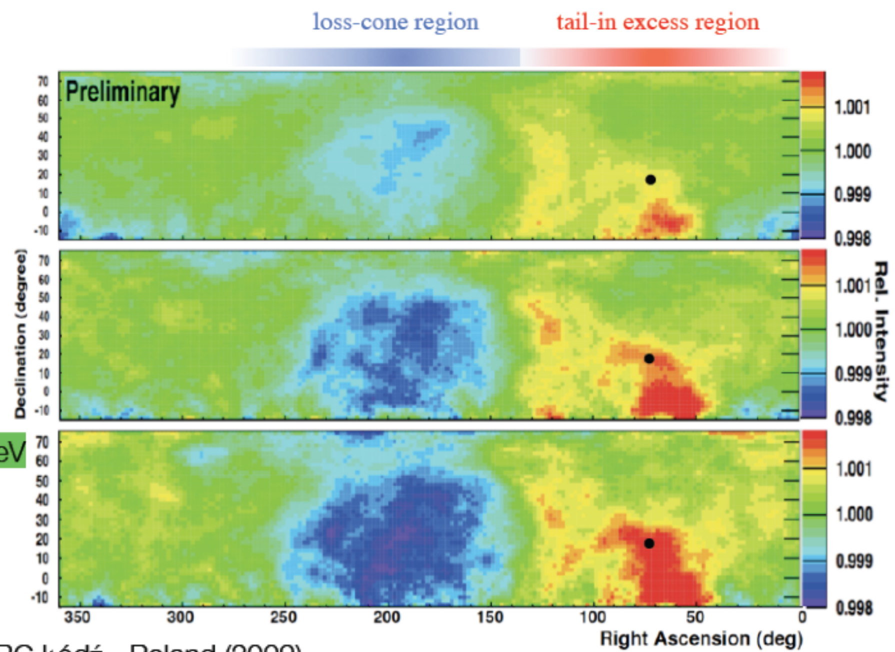

0.7 TeV

1.5 TeV

3.9 TeV

J.L. Zhang et al., 31st ICRC Łódź - Poland (2009)

Tibet-III

- data from 1997 to 2005
- 1874 days livetime
- $3.7 \cdot 10^{10}$ events
- angular resolution ~ 0.9°
- modal CR energy ~ 3 TeV

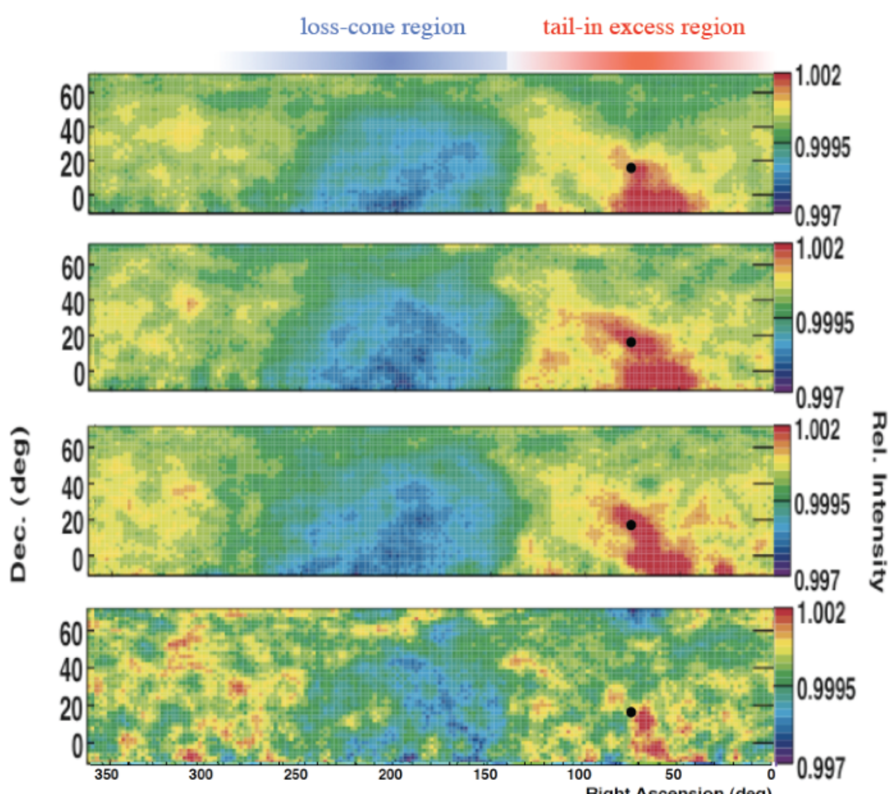

4 TeV

6.2 TeV

12 TeV

50 TeV

Amenomori et al., Science Vol. 314, pp. 439 (2006)

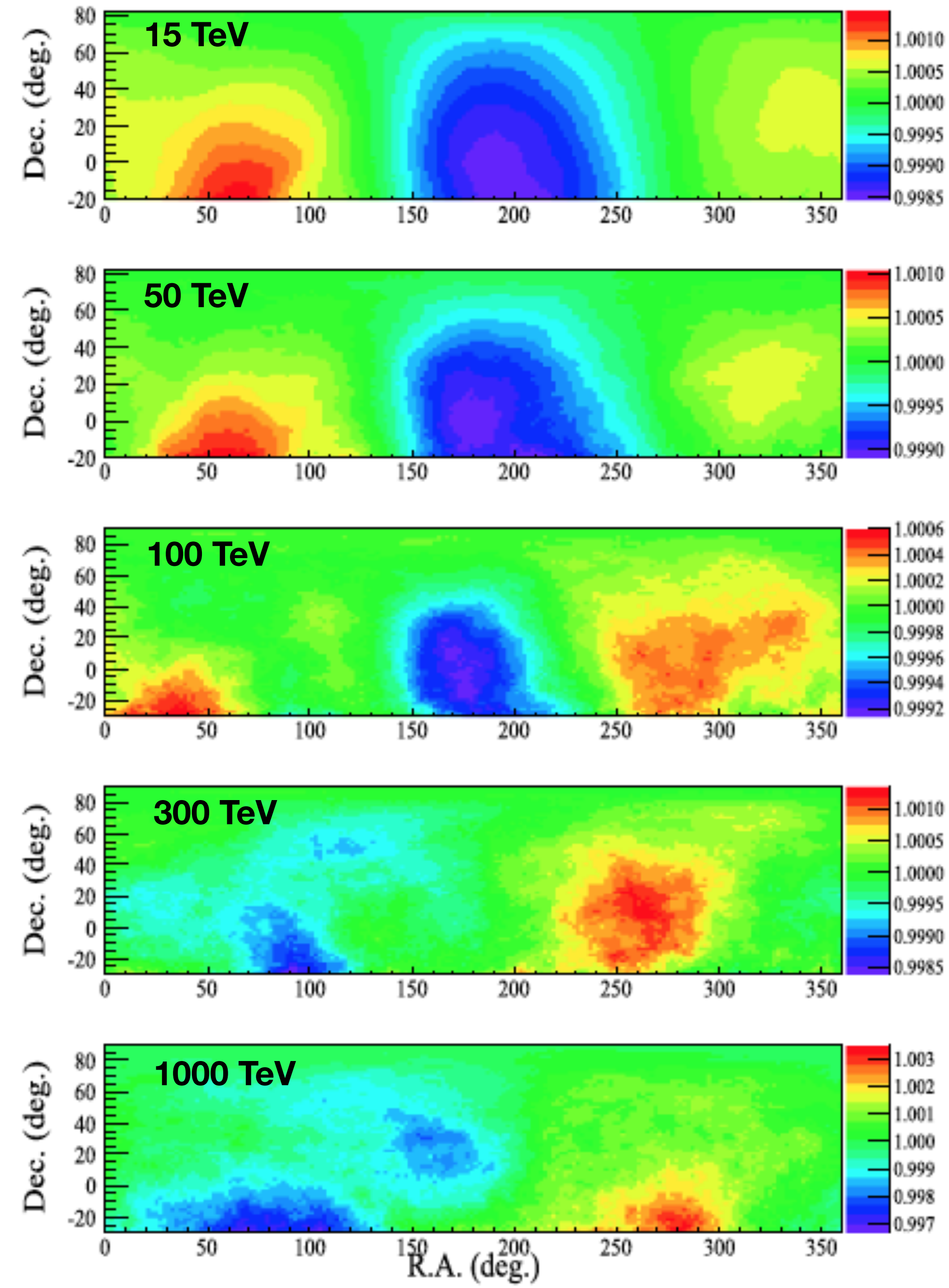

M. Amenomori, 2017ApJ…836..153A

ICECUBE & ICETOP

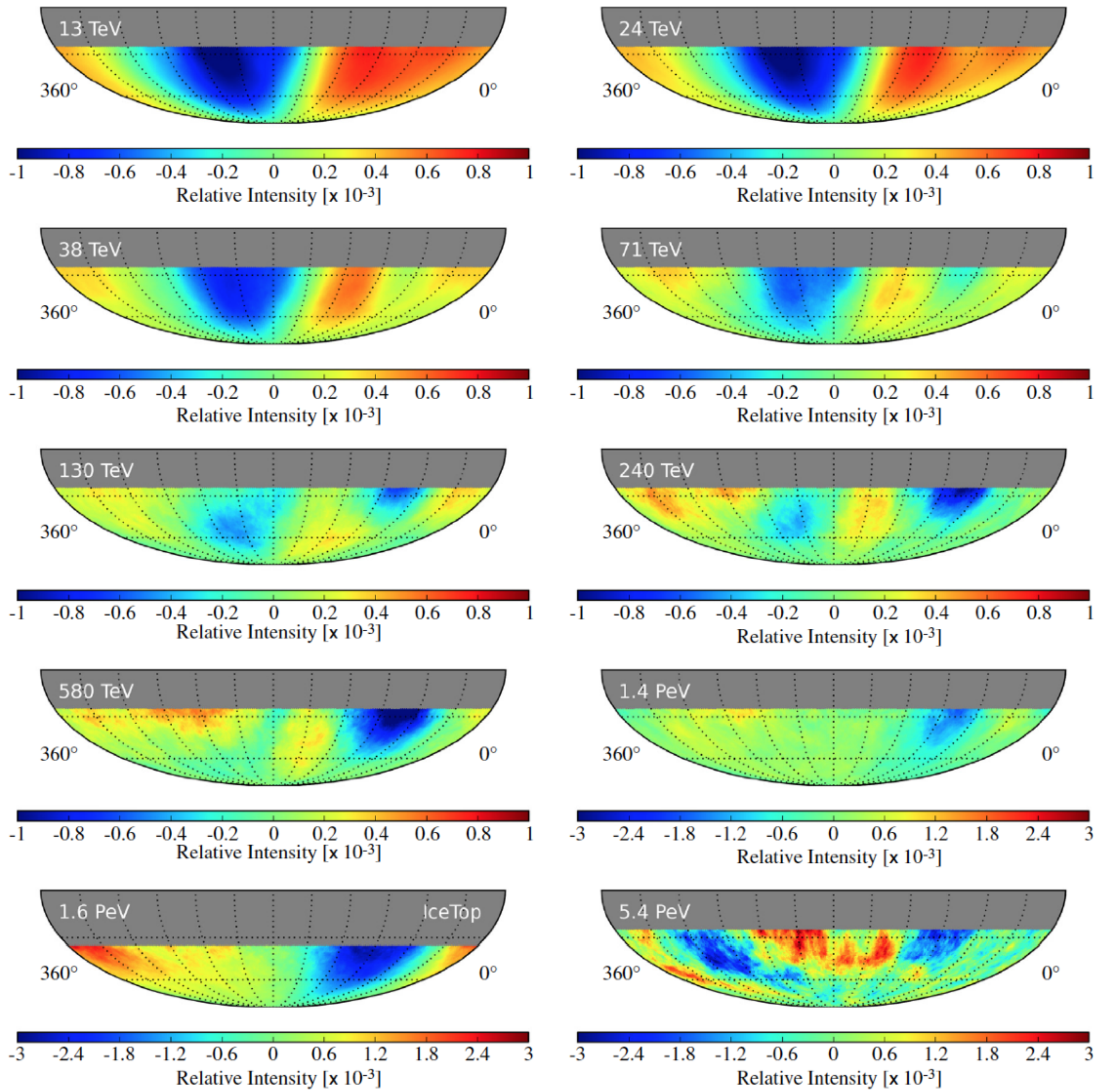

Anisotropy maps at different energies by IceCube and IceTop, Aartsen, et al., Astrophys. J. 826 (2016) 220.

Energy dependence of amplitude and phase

A_1

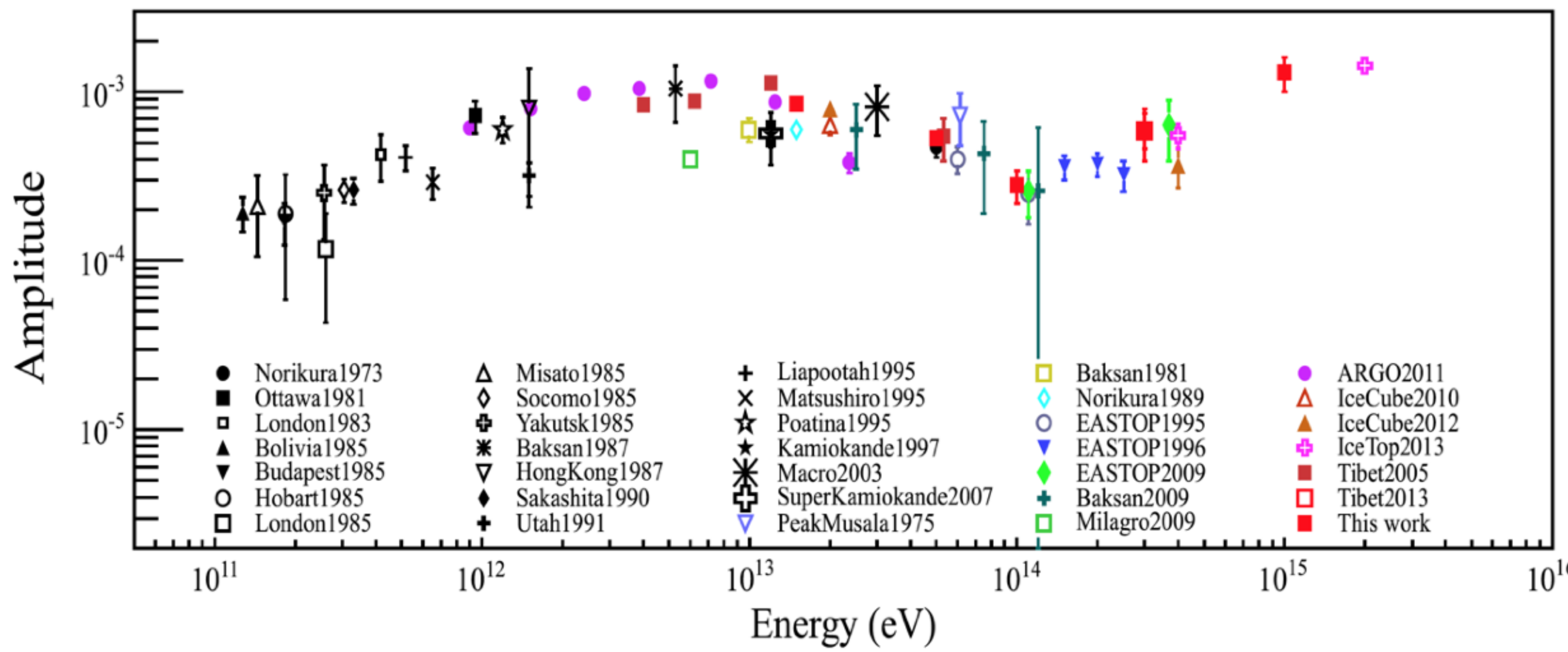

ϕ_1

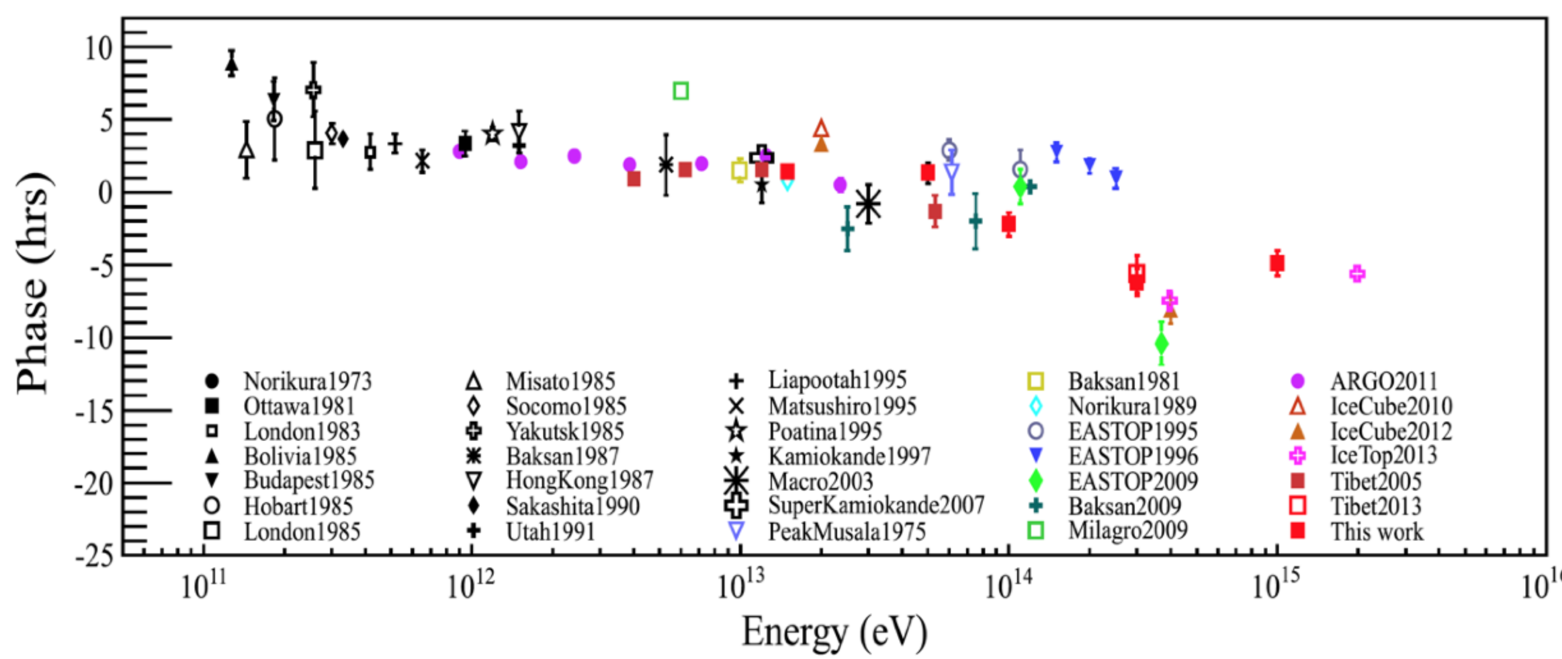

M. Amenomori, 2017ApJ…836..153A

$$R(\alpha) = 1 + A_1 \cos(\alpha - \phi_1)$$

$R(\alpha)$: the relative intensity of CRs at R.A.

Temporal Variations of anisotropy

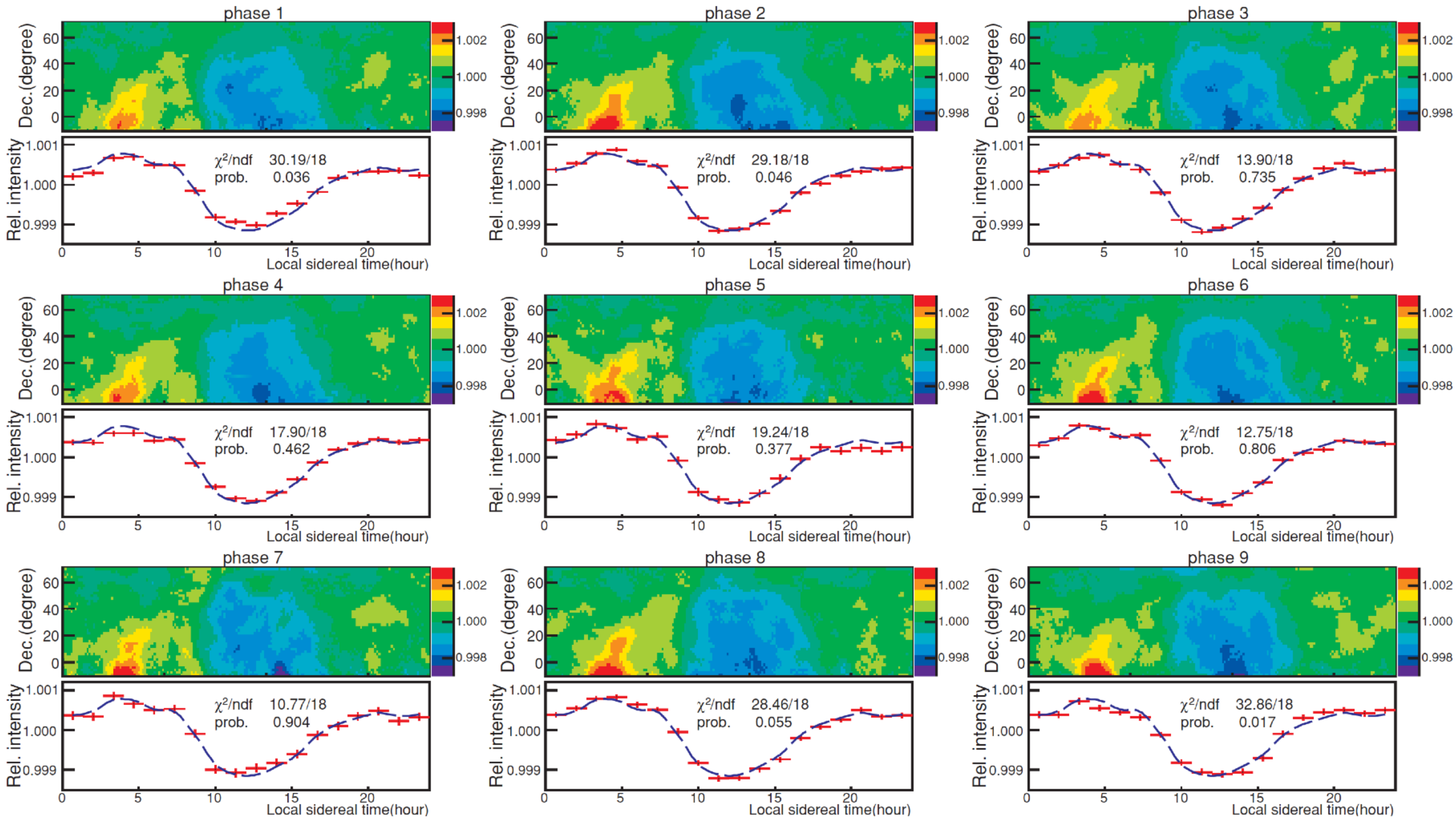

M. Amenomori, 2010ApJ...711..119A

CR intensity variation in the local sidereal time frame for CRs with the modal energy around 5 TeV in the nine phases of Tibet III array

Anisotropy of ultrahigh energy cosmic rays

COSMIC RAYS

Observation of a large-scale anisotropy in the arrival directions of cosmic rays above 8×10^{18} eV

The Pierre Auger Collaboration*†

Cosmic rays are atomic nuclei arriving from outer space that reach the highest energies observed in nature. Clues to their origin come from studying the distribution of their arrival directions. Using 3×10^4 cosmic rays with energies above 8×10^{18} electron volts, recorded with the Pierre Auger Observatory from a total exposure of 76,800 km^2 sr year, we determined the existence of anisotropy in arrival directions. The anisotropy, detected at more than a 5.2σ level of significance, can be described by a dipole with an amplitude of $6.5^{+1.3}_{-0.9}$ percent toward right ascension $\alpha_d = 100 \pm 10$ degrees and declination $\delta_d = -24^{+12}_{-13}$ degrees. That direction indicates an extragalactic origin for these ultrahigh-energy particles.

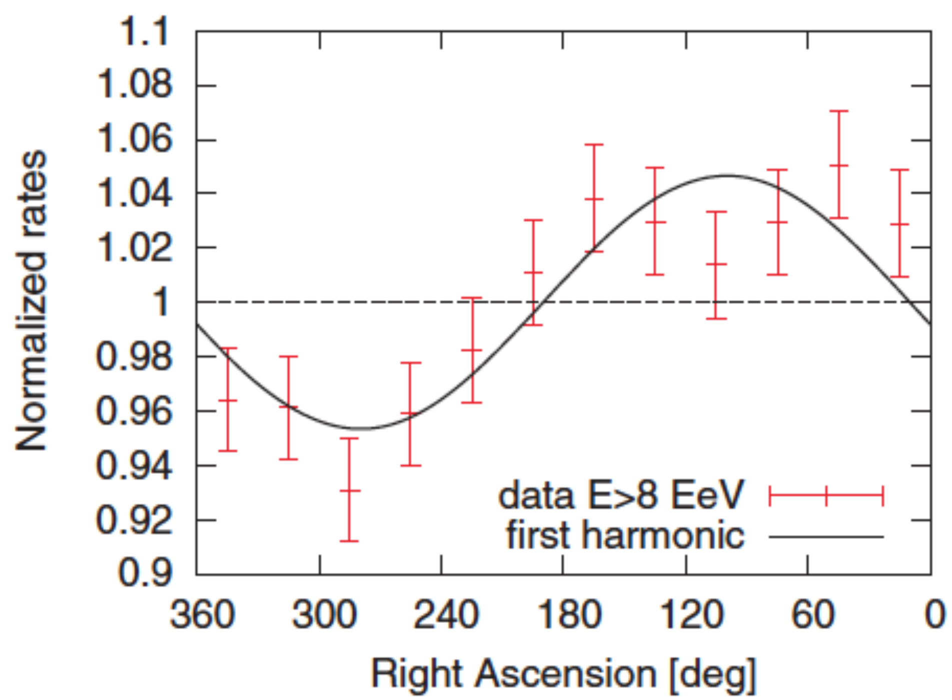

Normalized rate of events as a function of right ascension.

Equatorial coordinates

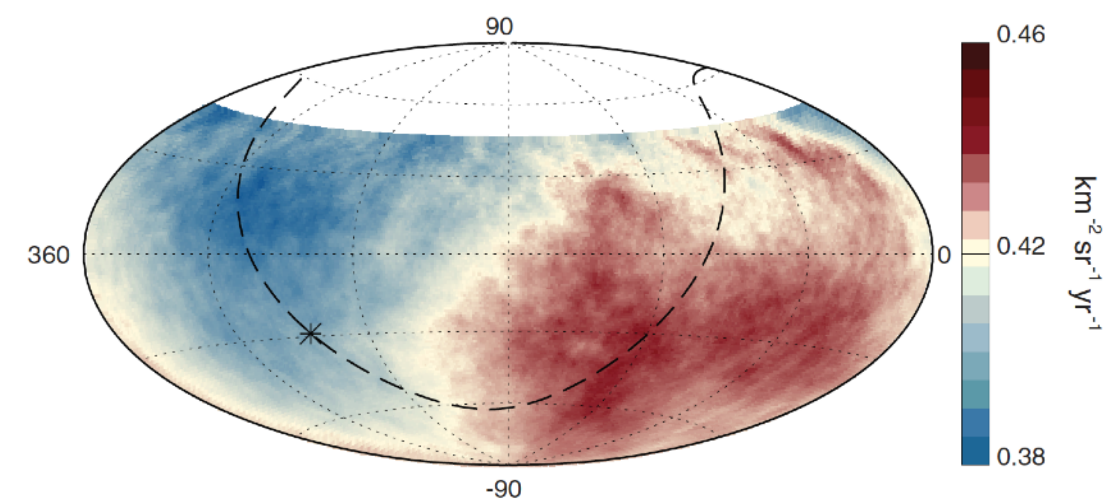

Galactic coordinates

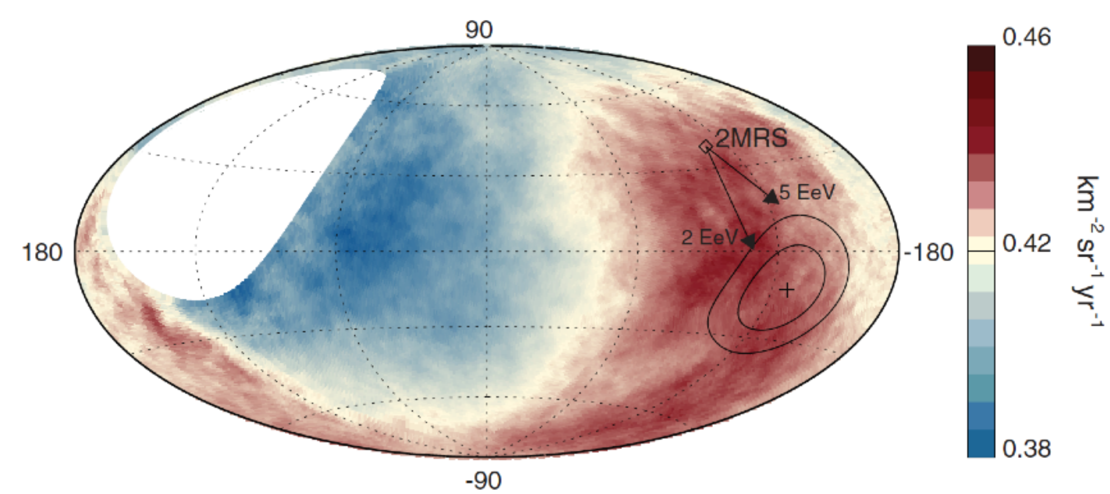

Possible origin of dipole anisotropy

Dipole anisotropy is defined as

$$\delta \equiv \frac{f_{\max} - f_{\min}}{f_{\max} + f_{\min}} = \frac{3\mathbf{K}}{v} \frac{\nabla n_{\rm CR}}{n_{\rm CR}}$$

Under the framework of isotropic diffusion,

$$K_{ij} \rightarrow K$$

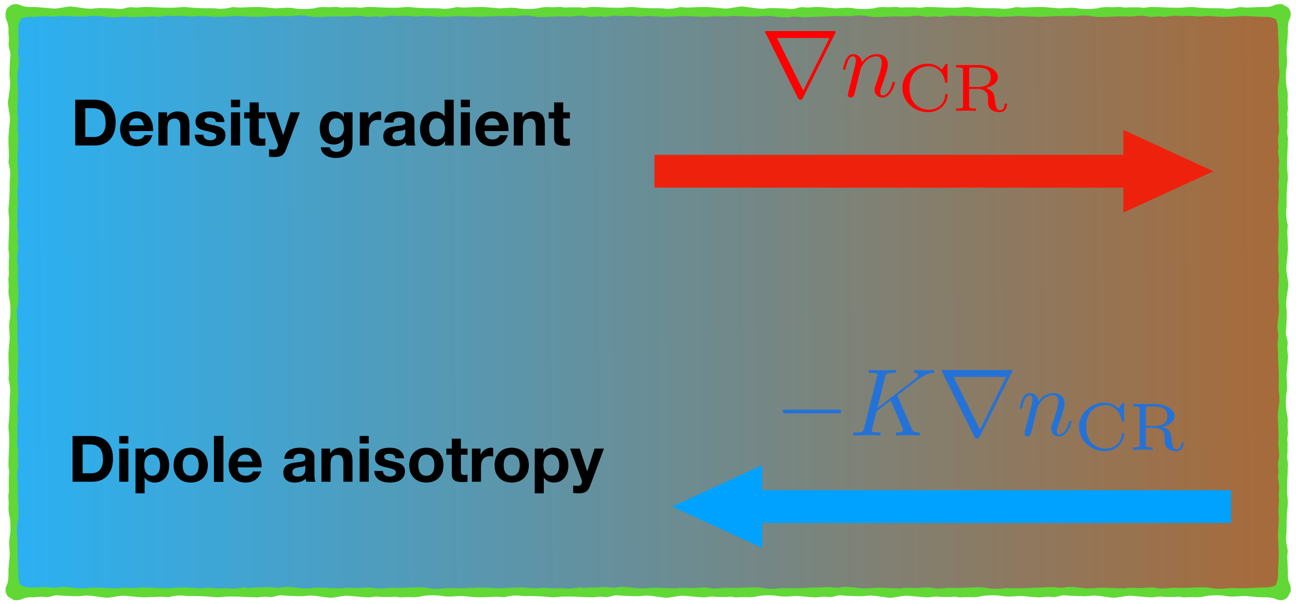

- Non-uniform distribution of sources [Blasi & Amato 12; Sveshnikova *et al.*13]
- Local sources [Liu, Bi, *et al.*17]
- Spatial-dependent diffusion [Guo, *et al.*16]
- Local magnetic field [Schwadron *et al.* 14; Mertsch & Funk 14]
- Compton-Getting effect [Compton & Getting 35]

In traditional transport model, diffusion is rigidity dependent,

$$K \propto R^{\delta}$$

Its power index is obtained by fitting the B/C data, Be10/Be9. At present, $\delta \sim 0.3 - 0.6$.

The magnitude of dipole anisotropy is predicted to gradually increase with energy.

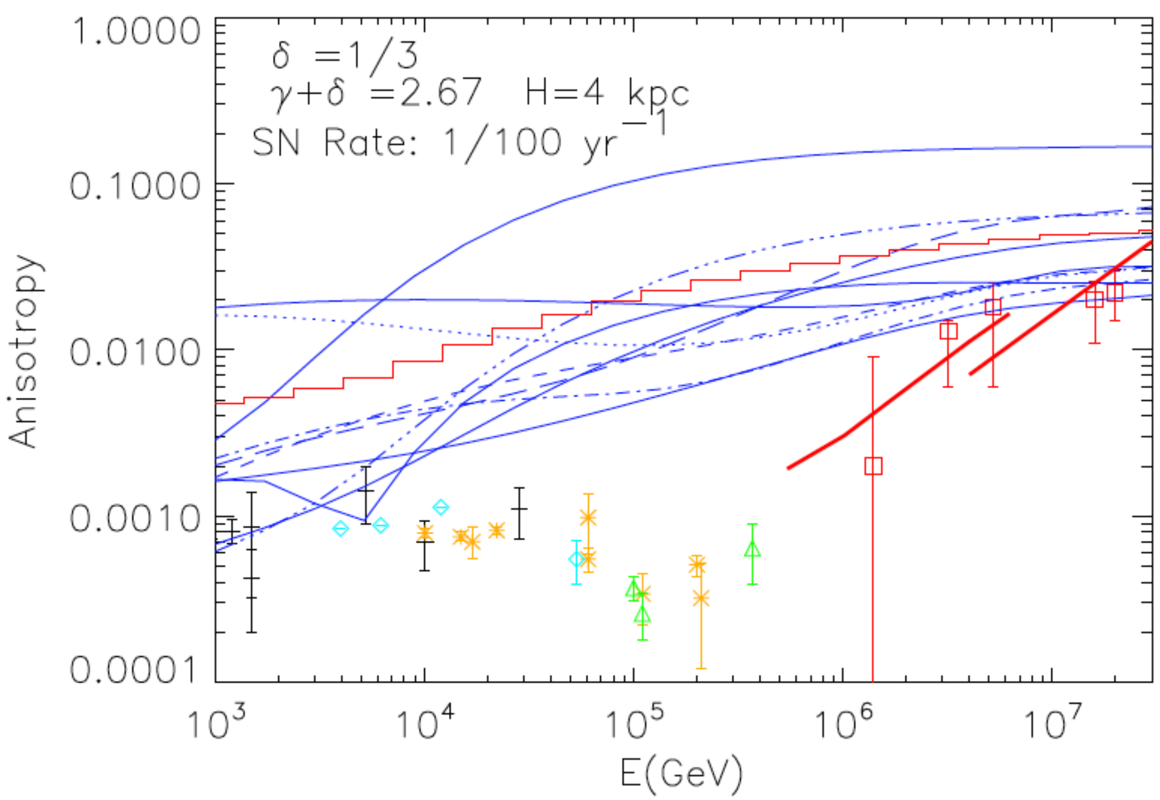

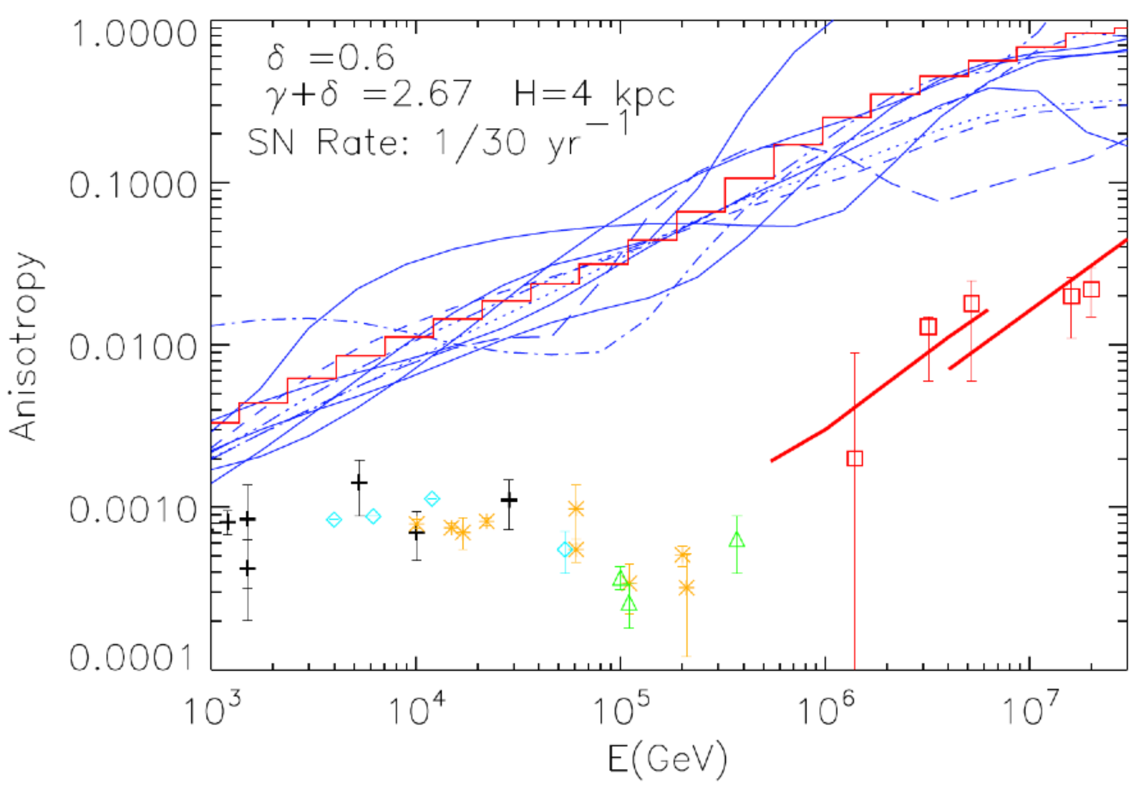

P. Blasi, E. Amato, 2012JCAP…01..011B

Despite that the magnitude of dipole anisotropy can be partially settled, the phase is difficult.

Spatial-dependent diffusion

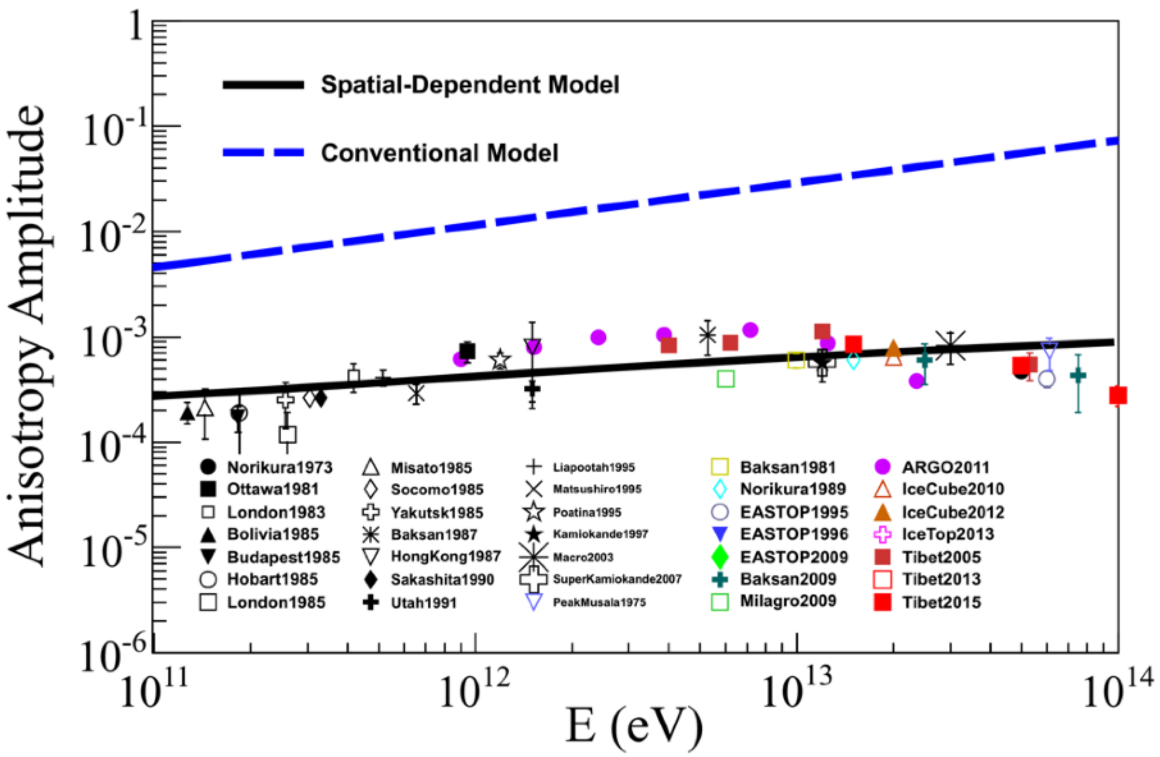

Y. Q. Guo, Z. Tian, and C. Jin, 2016ApJ…819...54G

Nearby source

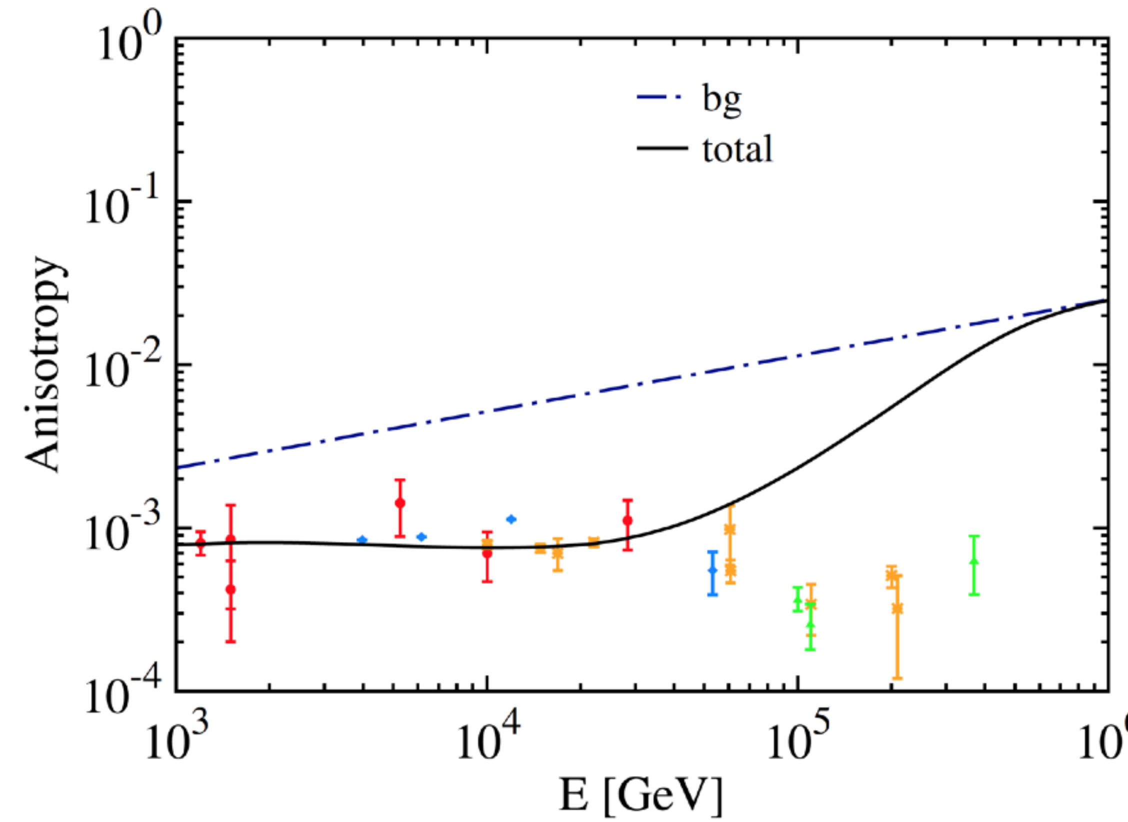

W. Liu, X. J. Bi, S. J. Lin, B. B. Wang, and P. F. Yin, 2017PhRvD..96b3006L

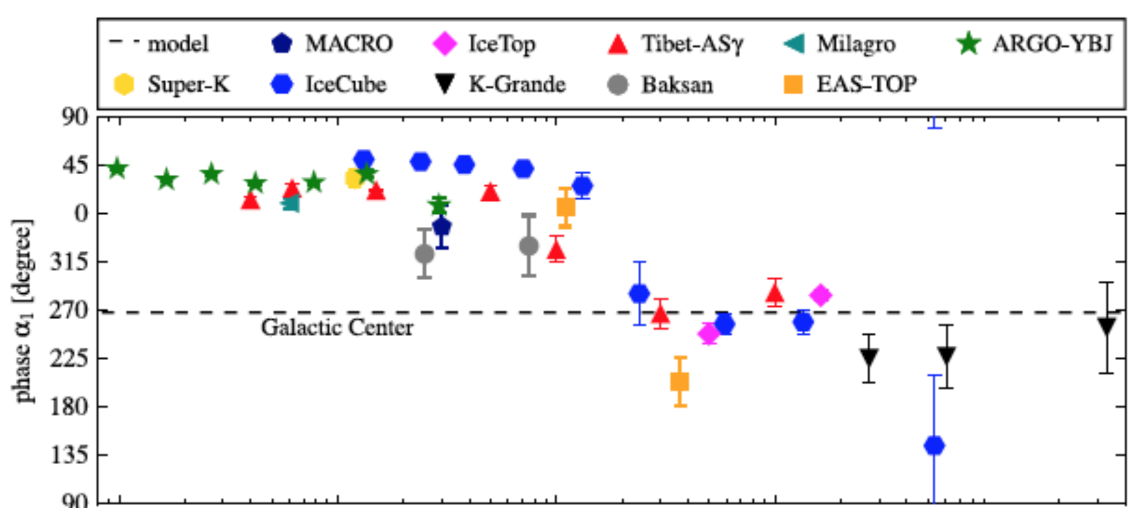

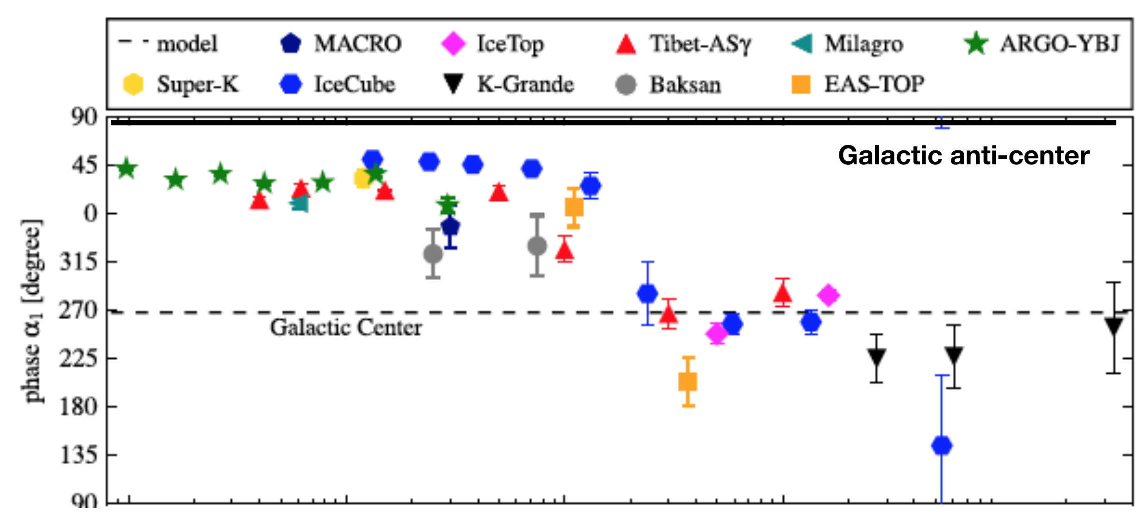

The region I points to the Cygnus, whose direction is parallel to the tangent line of spiral arm.

The region II points to the north pole, from galactic disk to halo. It is direction of cosmic ray diffusion.

Thus inferred from above observational results, the dipole anisotropy may connect with large-scale structure in the Galaxy, especially with regular magnetic field.

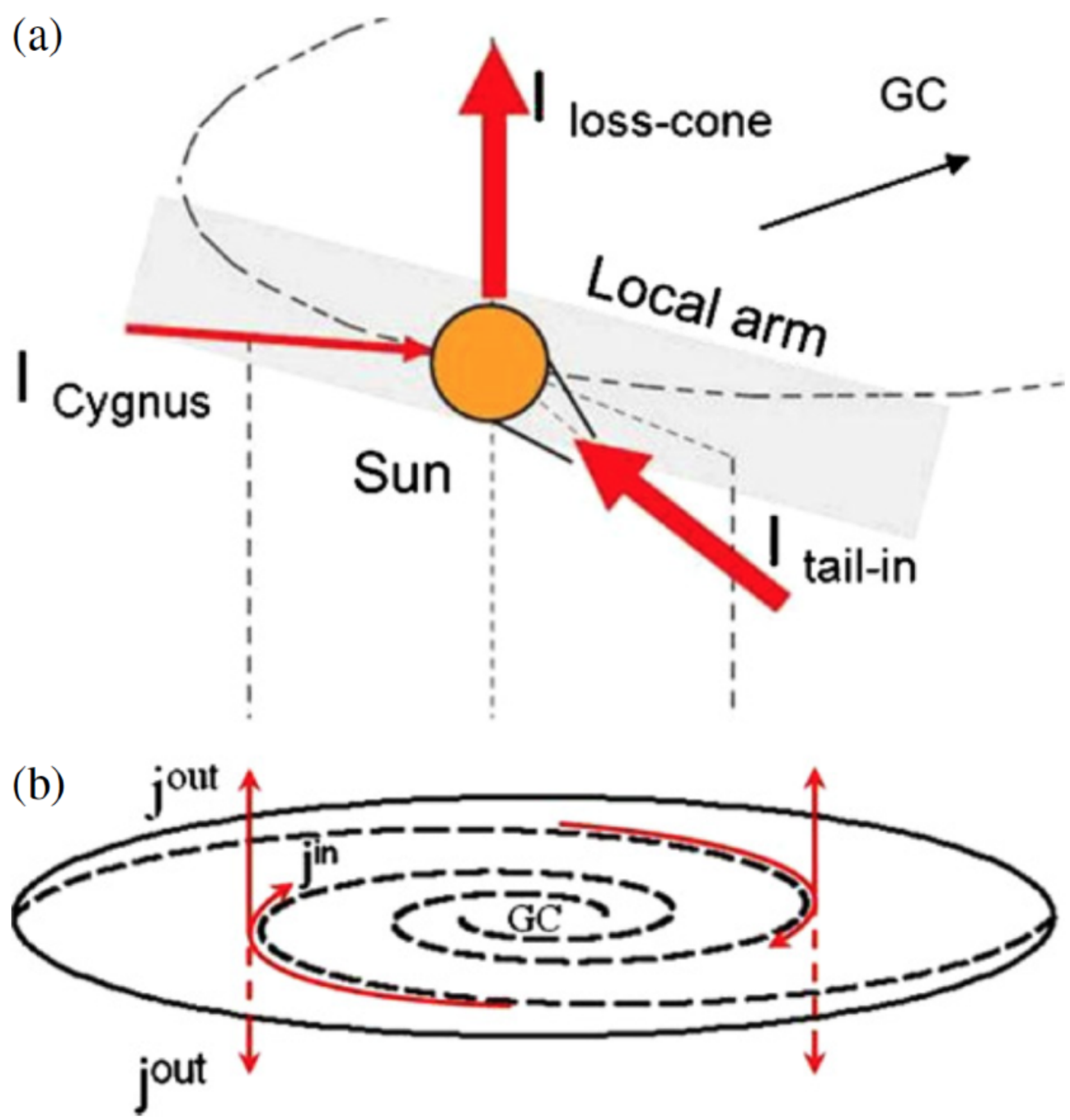

Large-scale Galactic Regular Magnetic Field

Observations of spiral galaxies find that there is large scale regular magnetic field along the spiral arms.

Ordered magnetic field also exists out to large distances from the plane, i.e. radio halos, with X-shaped patterns.

Our Milky Way is thought to be a barred spiral galaxy, with four major spiral arms.

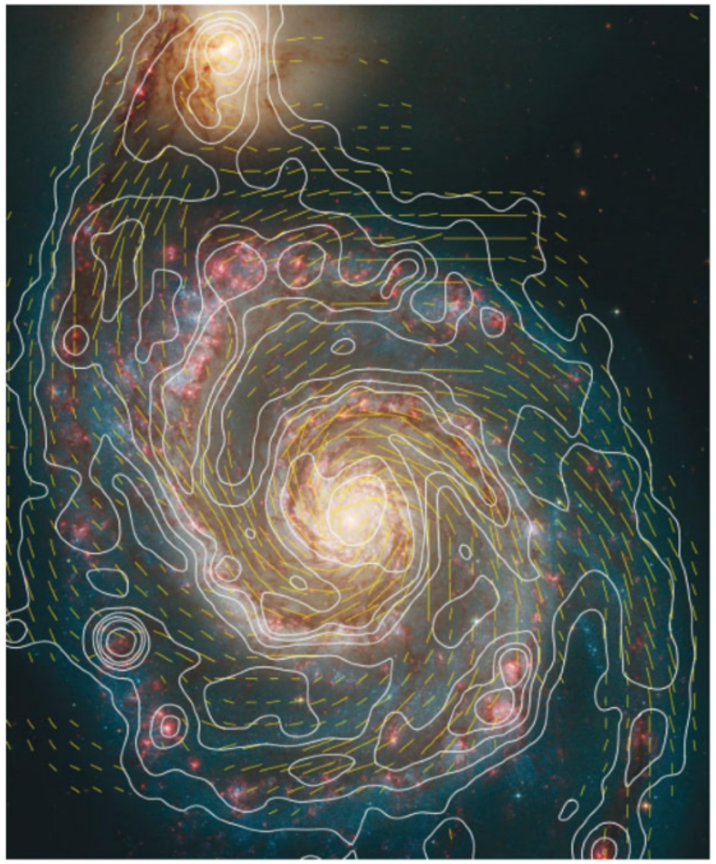

face-on galaxy M51 at 6.2 cm

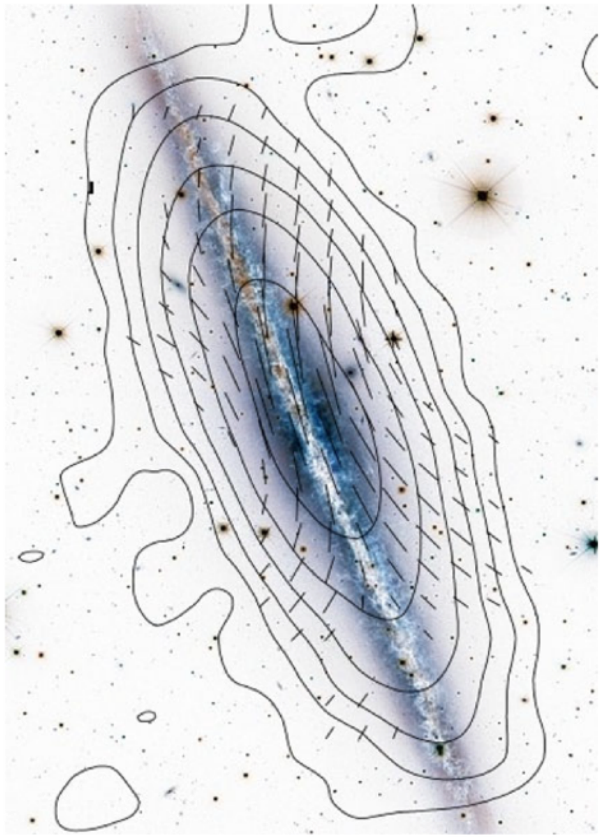

edge-on galaxy NGC 4631 at 3.6 cm

Galactic magnetic field consists of three components,

Toroidal fields in Galactic disk and halo

$$B_\phi^{\rm disk}(R,z) = \begin{cases} B_{D0}\, e^{-|z|/z_0} & (R < R_{cD}) \\ B_{D0}\, e^{-|z|/z_0}\, e^{-(R-R_\odot)/R_0} & (R > R_{cD}) \end{cases},$$

$$B_\phi^{\rm halo}(R,z) = B_{H0}\left[1+\left(\frac{|z|-z_0^H}{z_1^H}\right)\right]^{-1} \frac{R}{R_O^H}\, e^{\left(1-\frac{R}{R_0^H}\right)}$$

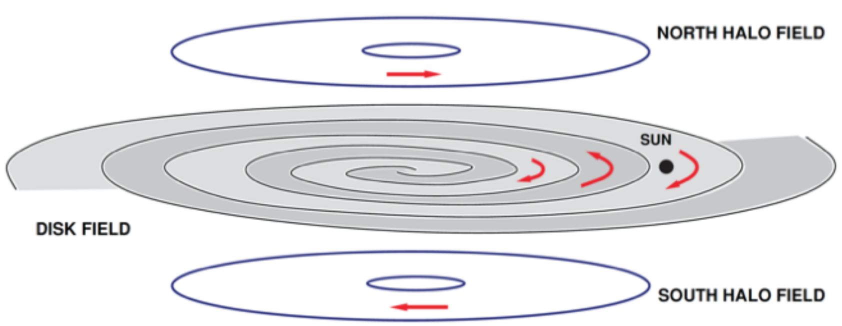

X. H. Sun, W. Reich, A. Waelkens, T. A. Enßlin, 2008A&A...477..573S; M. S. Pshirkov, et. al. 2011ApJ...738..192P

Poloidal fields

$$B_z^{\rm pol}(R,z) = B_{\rm X}(R,z)\cos\left[\Theta_{\rm X}(R,z)\right],$$

$$B_R^{\rm pol}(R,z) = B_{\rm X}(R,z)\sin\left[\Theta_{\rm X}(R,z)\right],$$

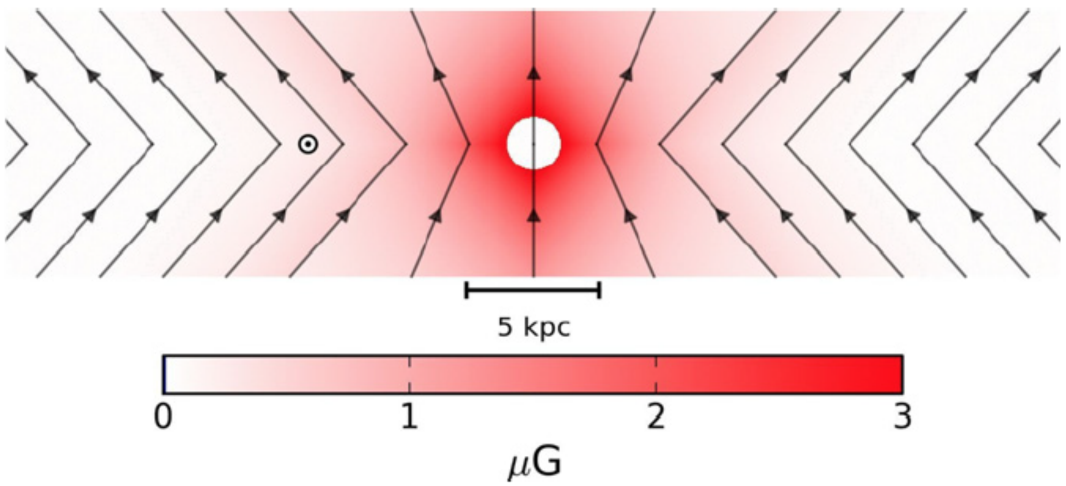

R. Jansson, G. R. Farrar, 2012ApJ…757...14J

Configuration of Galactic regular magnetic field

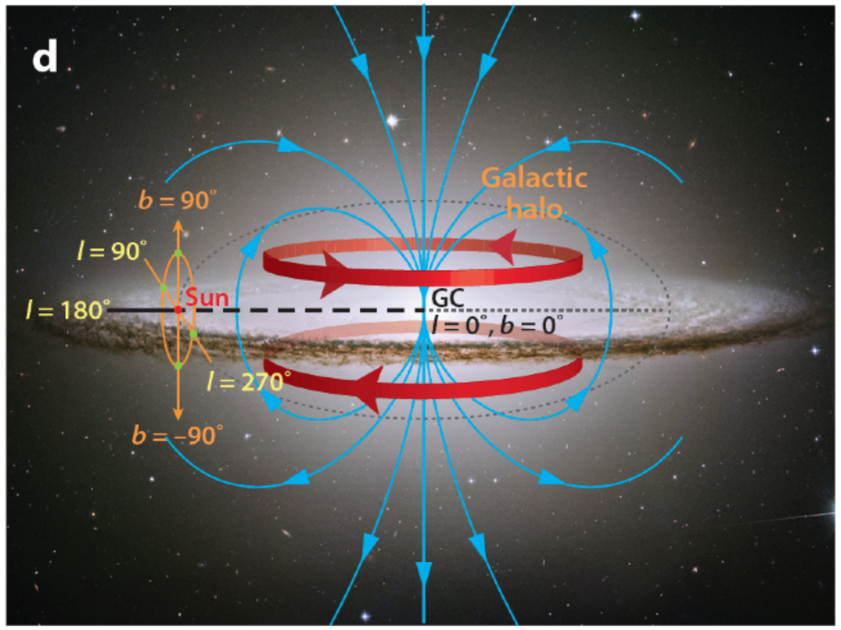

J. L. Han, 2017ARA&A..55..111H

Magnetic field induced by Cosmic ray flows

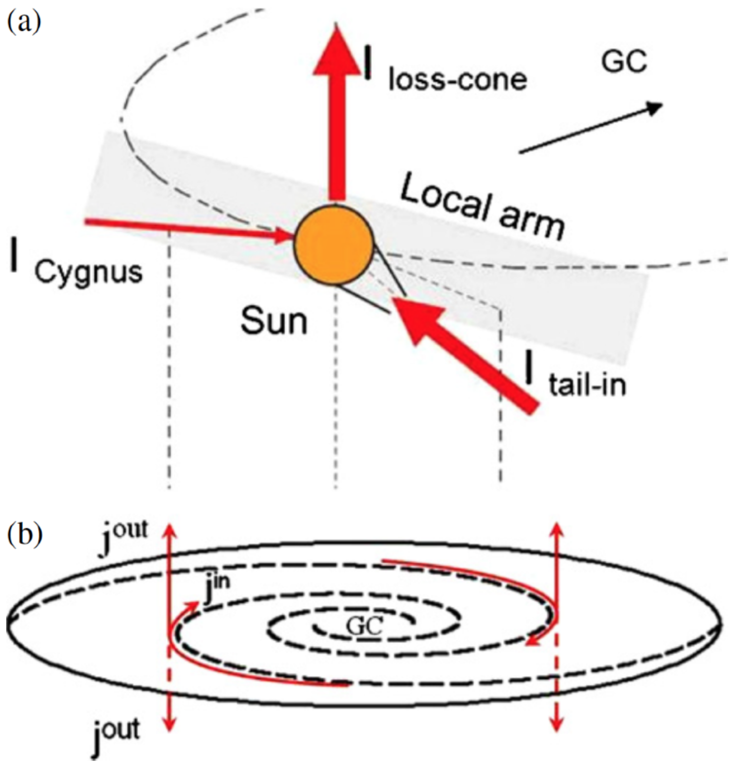

Extend the anisotropy image observed in the solar vicinity to the whole Galaxy.

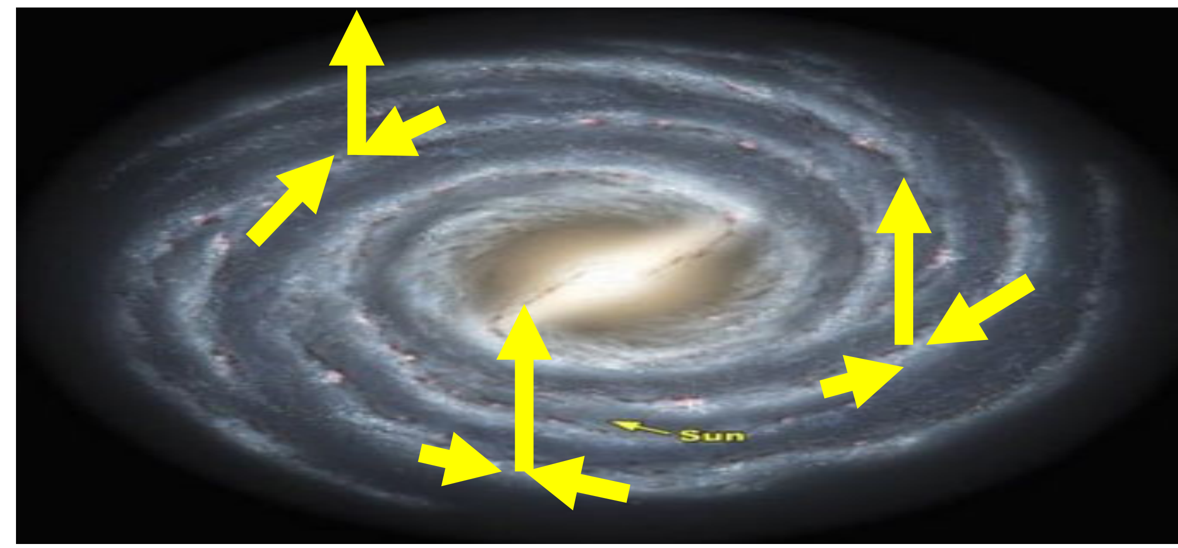

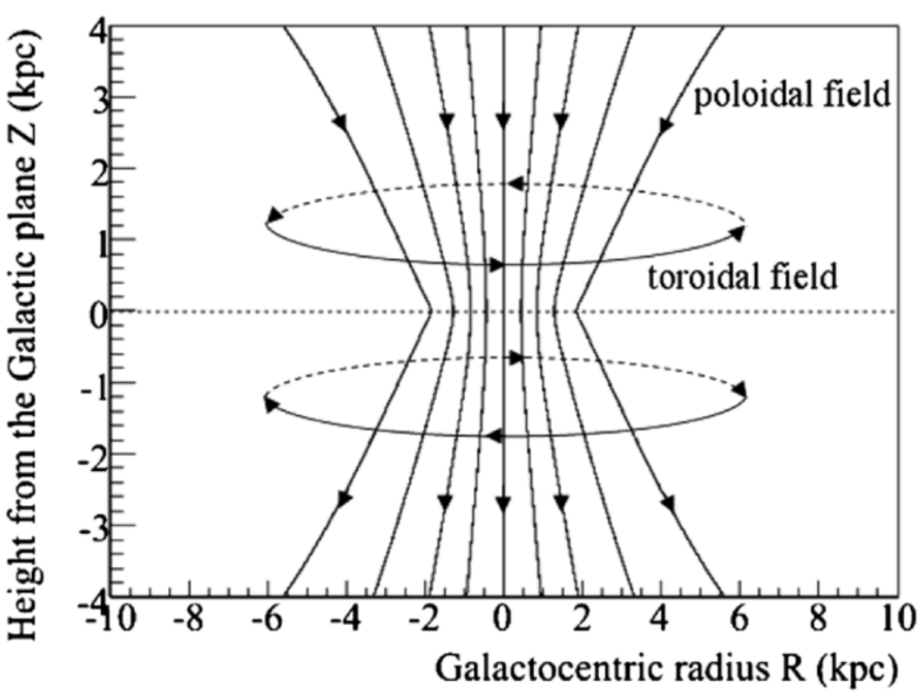

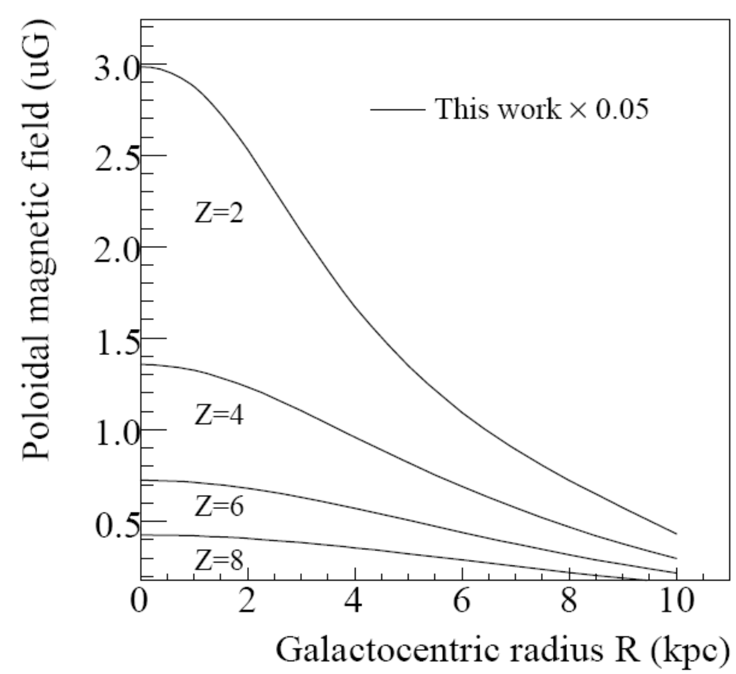

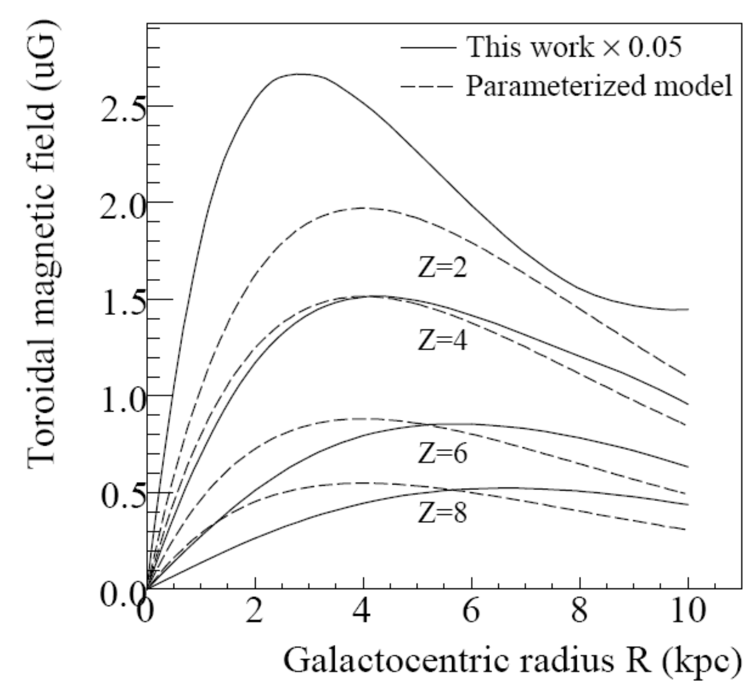

X. B. Qu, Y. Zhang, L. Xue, C. Liu, H. B. Hu, 2012ApJ…750L..17Q

Parameterized model: Sun, X. H. & Reich,W. 2010, Research in Astronomy and Astrophysics, 10, 1287

Cosmic ray anisotropic diffusion

- Traditional numerical packages, e.g. GALPROP, DRAGON-1, PICARD, assume the isotropic diffusion coefficient.

Diffusion equation

n = CR density per unit of p at $\vec{r}$

$$\frac{\partial n(\vec{r},p,t)}{\partial t} = q(\vec{r},p)$$

sources (SNR, nuclear reactions...)

Diffusion

$$+\boxed{\vec{\nabla}\cdot[D_{xx}\vec{\nabla}n} - \vec{V}n]$$

Diffusive reacceleration

(diffusion in the momentum space)

$$+\frac{\partial}{\partial p}\left[p^2 D_{pp}\frac{\partial}{\partial p}\frac{n}{p^2}\right]$$

convection

(Galactic wind)

E-loss

$$-\frac{\partial}{\partial p}\left[\frac{dp}{dt}n - \frac{1}{3}p\vec{\nabla}\cdot\vec{V}n\right]$$

fragmentation

$$-\frac{n}{\tau_f} - \frac{n}{\tau_d}$$

radioactive decay

+ boundary conditions

Diffusion tensor is only diagonal,

$$\kappa'_{\mu\nu} = \begin{pmatrix} D_{xx}(x,y,z) & 0 & 0 \\ 0 & D_{yy}(x,y,z) & 0 \\ 0 & 0 & D_{zz}(x,y,z) \end{pmatrix}$$

- When large-scale regular magnetic field is involved, the whole diffusion tensor has to be considered. Since the diffusion tensor contains the off-diagonal elements,

$$\kappa = \begin{pmatrix} D_{xx} & D_{xy} & D_{xz} \\ D_{yx} & D_{yy} & D_{yz} \\ D_{zx} & D_{zy} & D_{zz} \end{pmatrix}$$

- the diffusion term turns out to be

$$\begin{aligned}
\nabla \cdot (\kappa \cdot \nabla \psi) \rightarrow\ & D_{xx}\frac{\partial^2 \psi}{\partial x^2} + D_{yy}\frac{\partial^2 \psi}{\partial y^2} + D_{zz}\frac{\partial^2 \psi}{\partial z^2} + \frac{\partial D_{xx}}{\partial x}\frac{\partial \psi}{\partial x} + \frac{\partial D_{yy}}{\partial y}\frac{\partial \psi}{\partial y} + \frac{\partial D_{zz}}{\partial z}\frac{\partial \psi}{\partial z} \\
& + D_{xy}\frac{\partial^2 \psi}{\partial x \partial y} + D_{xz}\frac{\partial^2 \psi}{\partial x \partial z} + D_{yz}\frac{\partial^2 \psi}{\partial y \partial z} + \frac{\partial D_{xy}}{\partial x}\frac{\partial \psi}{\partial y} + \frac{\partial D_{xz}}{\partial x}\frac{\partial \psi}{\partial z} + \frac{\partial D_{yz}}{\partial y}\frac{\partial \psi}{\partial z} \\
& + D_{yx}\frac{\partial^2 \psi}{\partial y \partial x} + D_{zx}\frac{\partial^2 \psi}{\partial z \partial x} + D_{zy}\frac{\partial^2 \psi}{\partial z \partial y} + \frac{\partial D_{yx}}{\partial y}\frac{\partial \psi}{\partial x} + \frac{\partial D_{zx}}{\partial z}\frac{\partial \psi}{\partial x} + \frac{\partial D_{zy}}{\partial z}\frac{\partial \psi}{\partial y}
\end{aligned}$$

Each component of diffusion tensor is evaluated by

$$\boxed{D_{ij} \equiv D_\perp \delta_{ij} + (D_\parallel - D_\perp) b_i b_j \,, \qquad b_i \equiv \frac{B_i}{|\mathbf{B}|} \,,}$$

$$\boxed{D_\parallel = D_{0\parallel} \left(\frac{p}{Z}\right)^{\delta_\parallel} \quad \text{and} \quad D_\perp = D_{0\perp} \left(\frac{p}{Z}\right)^{\delta_\perp} \equiv \epsilon_D \, D_{0\parallel} \left(\frac{p}{Z}\right)^{\delta_\perp} \,,}$$

$D_\parallel$ and $D_\perp$ are the components of the diffusion tensor parallel and perpendicular to the mean magnetic field.

To solve the diffusion equation with off-diagonal elements still by Galprop, a new iteration method has been introduced, in which the off-diagonal elements are treated as injection term. The diffusion equation becomes

$$\frac{\partial \psi}{\partial t} - \frac{\partial}{\partial x}\left(D_{xx}\frac{\partial \psi}{\partial x}\right) - \frac{\partial}{\partial y}\left(D_{yy}\frac{\partial \psi}{\partial y}\right) - \frac{\partial}{\partial z}\left(D_{zz}\frac{\partial \psi}{\partial z}\right) = Q'(\boldsymbol{r}, p, t) \,,$$

$$\begin{aligned} Q'(\boldsymbol{r}, p, t) = Q(\boldsymbol{r}, p, t) & \\ & + D_{xy}\frac{\partial^2 \psi}{\partial x \partial y} + D_{xz}\frac{\partial^2 \psi}{\partial x \partial z} + D_{yz}\frac{\partial^2 \psi}{\partial y \partial z} + \frac{\partial D_{xy}}{\partial x}\frac{\partial \psi}{\partial y} + \frac{\partial D_{xz}}{\partial x}\frac{\partial \psi}{\partial z} + \frac{\partial D_{yz}}{\partial y}\frac{\partial \psi}{\partial z} \\ & + D_{yx}\frac{\partial^2 \psi}{\partial y \partial x} + D_{zx}\frac{\partial^2 \psi}{\partial z \partial x} + D_{zy}\frac{\partial^2 \psi}{\partial z \partial y} + \frac{\partial D_{yx}}{\partial y}\frac{\partial \psi}{\partial x} + \frac{\partial D_{zx}}{\partial z}\frac{\partial \psi}{\partial x} + \frac{\partial D_{zy}}{\partial z}\frac{\partial \psi}{\partial y} \end{aligned}$$

Iteration process

$$\frac{\partial \psi^{(0)}}{\partial t} - \frac{\partial}{\partial x}\left(D_{xx}\frac{\partial \psi^{(0)}}{\partial x}\right) - \frac{\partial}{\partial y}\left(D_{yy}\frac{\partial \psi^{(0)}}{\partial y}\right) = Q^{(0)}$$

$$\frac{\partial \psi^{(1)}}{\partial t} - \frac{\partial}{\partial x}\left(D_{xx}\frac{\partial \psi^{(1)}}{\partial x}\right) - \frac{\partial}{\partial y}\left(D_{yy}\frac{\partial \psi^{(1)}}{\partial y}\right) = Q^{(0)}$$

$$\frac{\partial \psi^{(2)}}{\partial t} - \frac{\partial}{\partial x}\left(D_{xx}\frac{\partial \psi^{(2)}}{\partial x}\right) - \frac{\partial}{\partial y}\left(D_{yy}\frac{\partial \psi^{(2)}}{\partial y}\right) = Q^{(1)}$$

$$\vdots$$

$$\vdots$$

$$\frac{\partial \psi^{(n+1)}}{\partial t} - \frac{\partial}{\partial x}\left(D_{xx}\frac{\partial \psi^{(n+1)}}{\partial x}\right) - \frac{\partial}{\partial y}\left(D_{yy}\frac{\partial \psi^{(n+1)}}{\partial y}\right) = Q^{(n)}$$

The whole computation is over when $Q^{(n-1)} = Q^{(n)}$.

Results

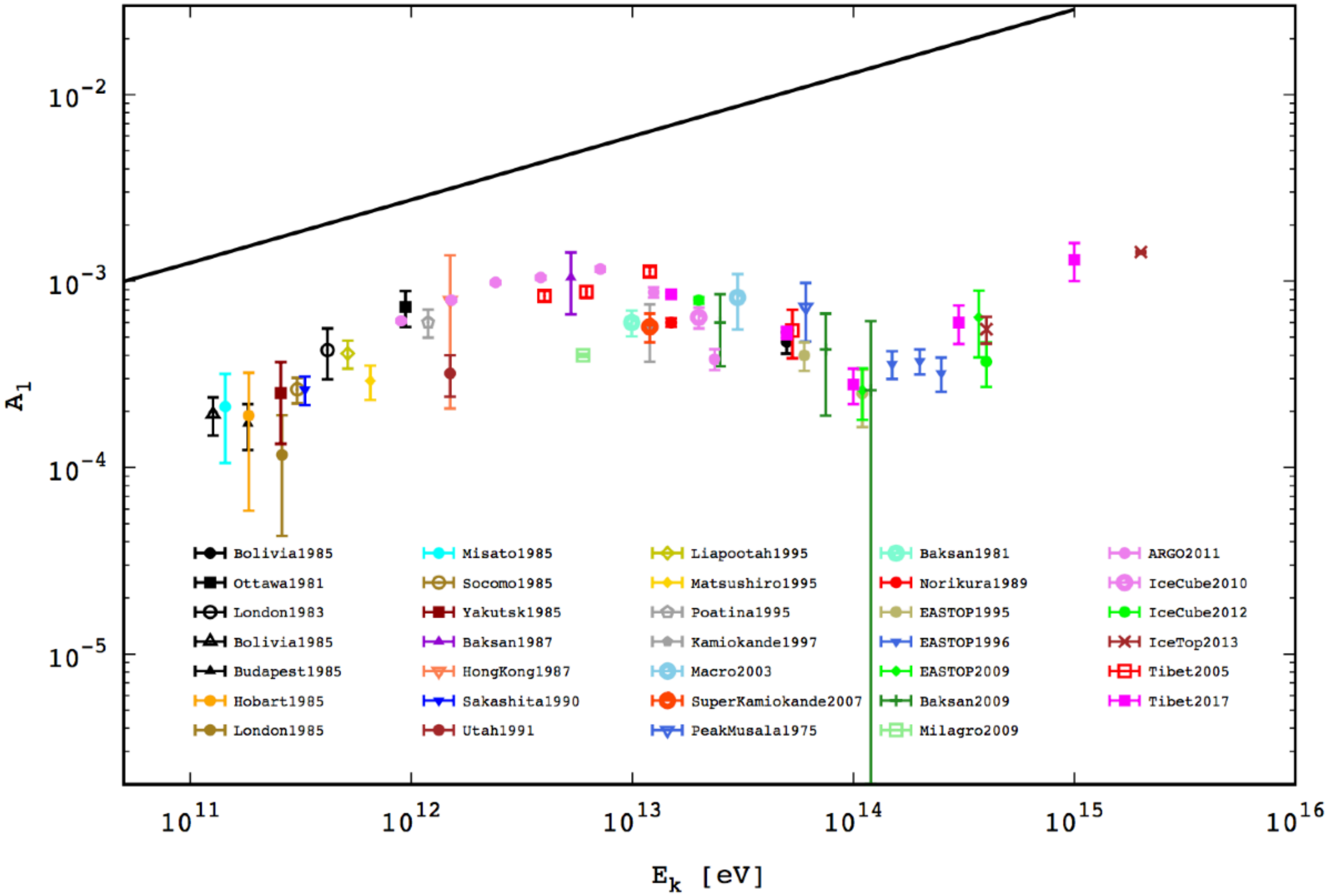

$$D_{\perp} = 5.9 \times 10^{28} \ \mathrm{cm}^2/s$$

$$D_{0\|} = 100 \ D_{0\perp}$$

$$\delta_{\|} = \delta_{\perp} = 0.34$$

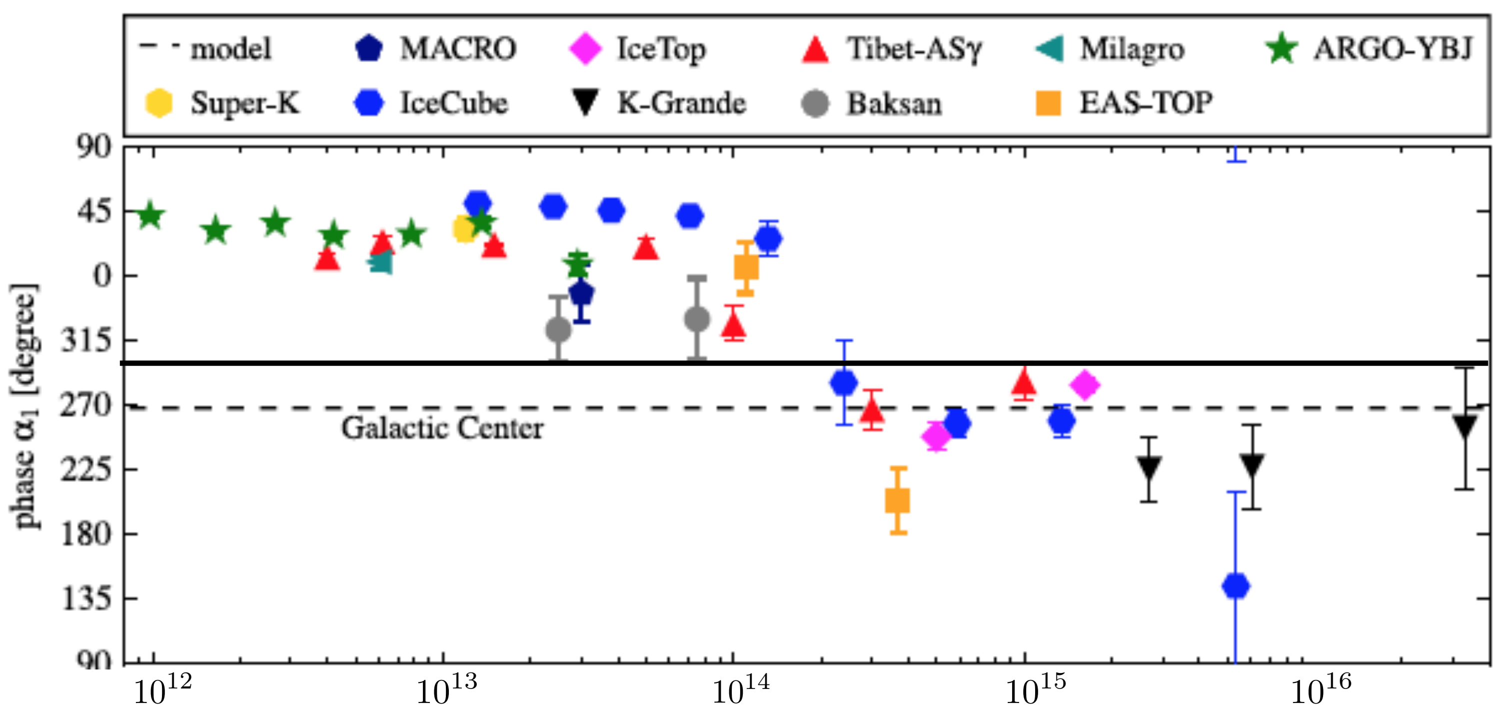

The phase is close to the Cygnus region.

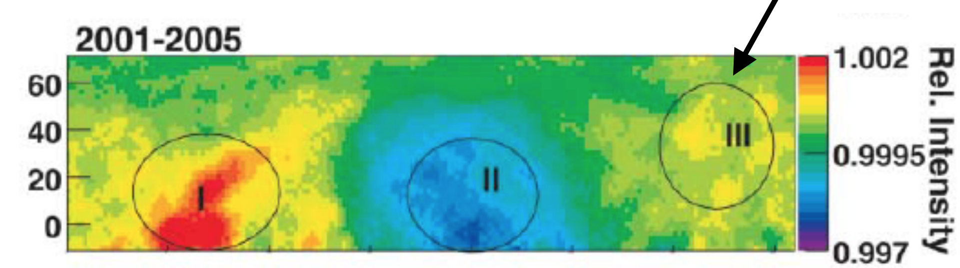

At lower energy, the stronger anisotropy comes from tail-in region, which may originate from solar magnetic field.

Summary

- There are dipole anisotropy of arrival directions of Galactic cosmic rays.
- Inferred from the arrival distribution, the dipole anisotropy may be induced by the large-scale regular magnetic field.
- A iteration algorithm has been implemented to solve transport equation allowing for the anisotropic diffusion.
- The amplitude and phase of dipole anisotropy are elementarily computed, which is going to be evaluated in-deep.

谢谢

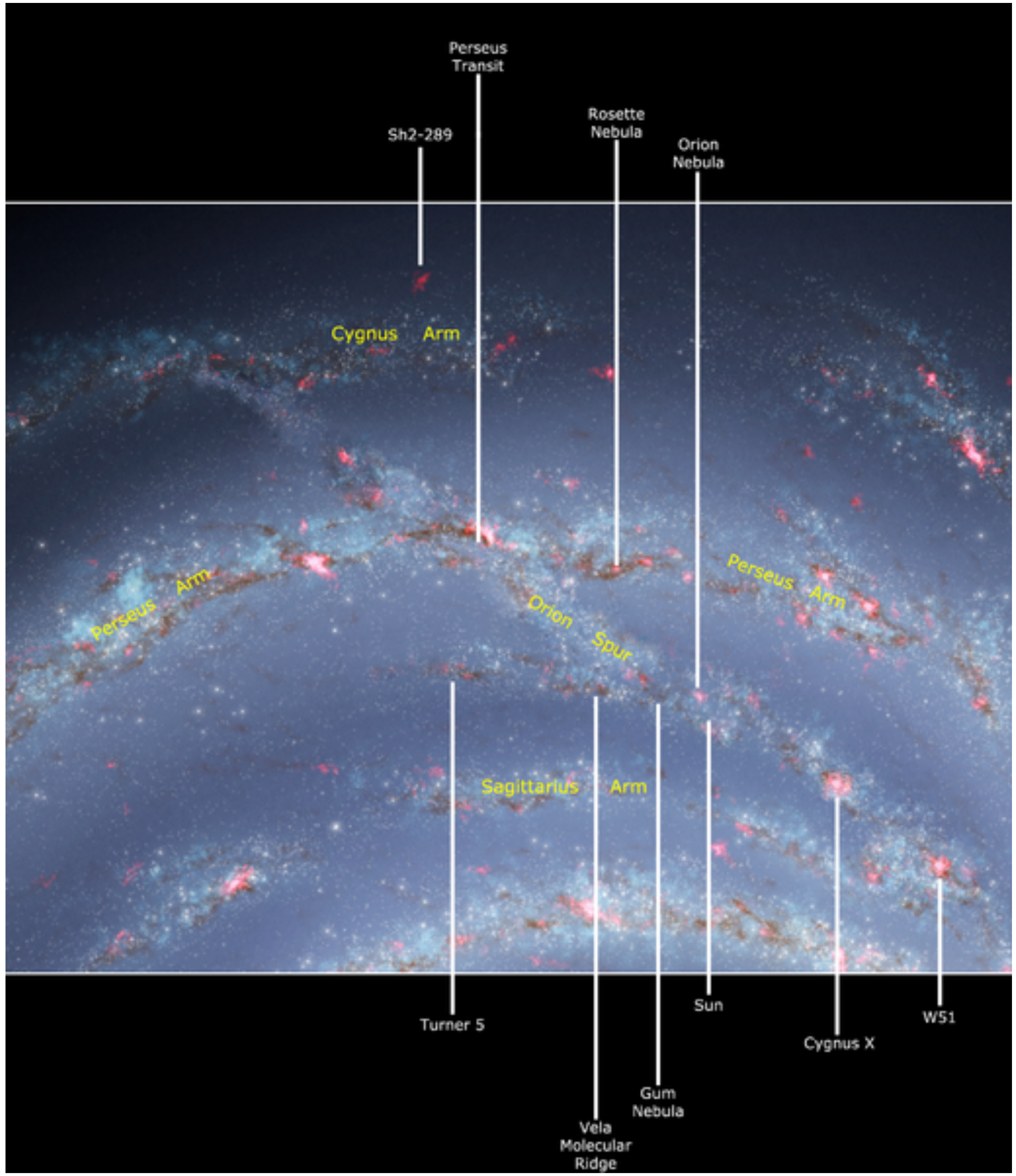
Perseus Transit
Sh2-289
Rosette Nebula
Orion Nebula
Cygnus Arm
Perseus Arm
Orion Spur
Perseus Arm
Sagittarius Arm
Turner 5
Vela Molecular Ridge
Gum Nebula
Sun
Cygnus X
W51

Radial distribution

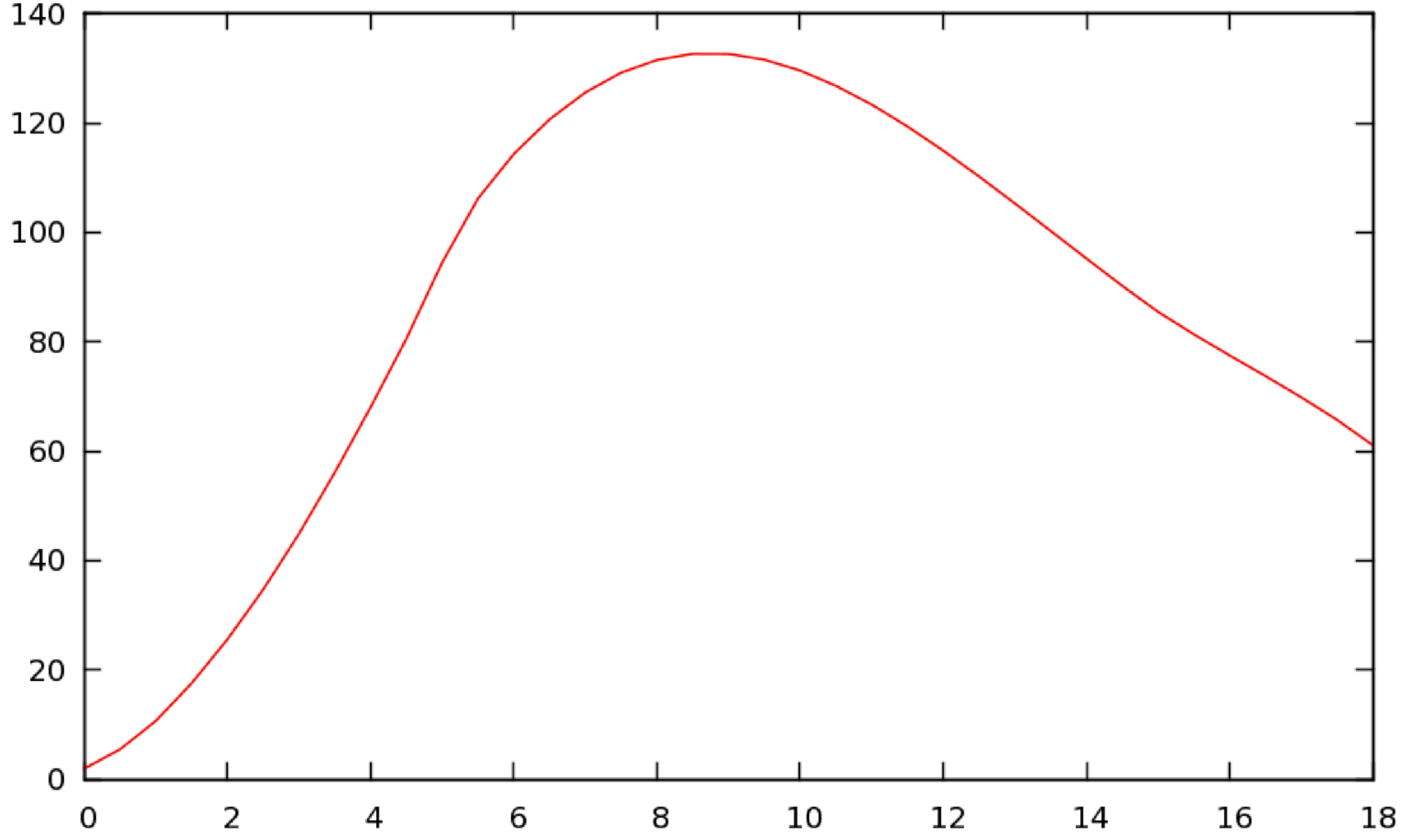

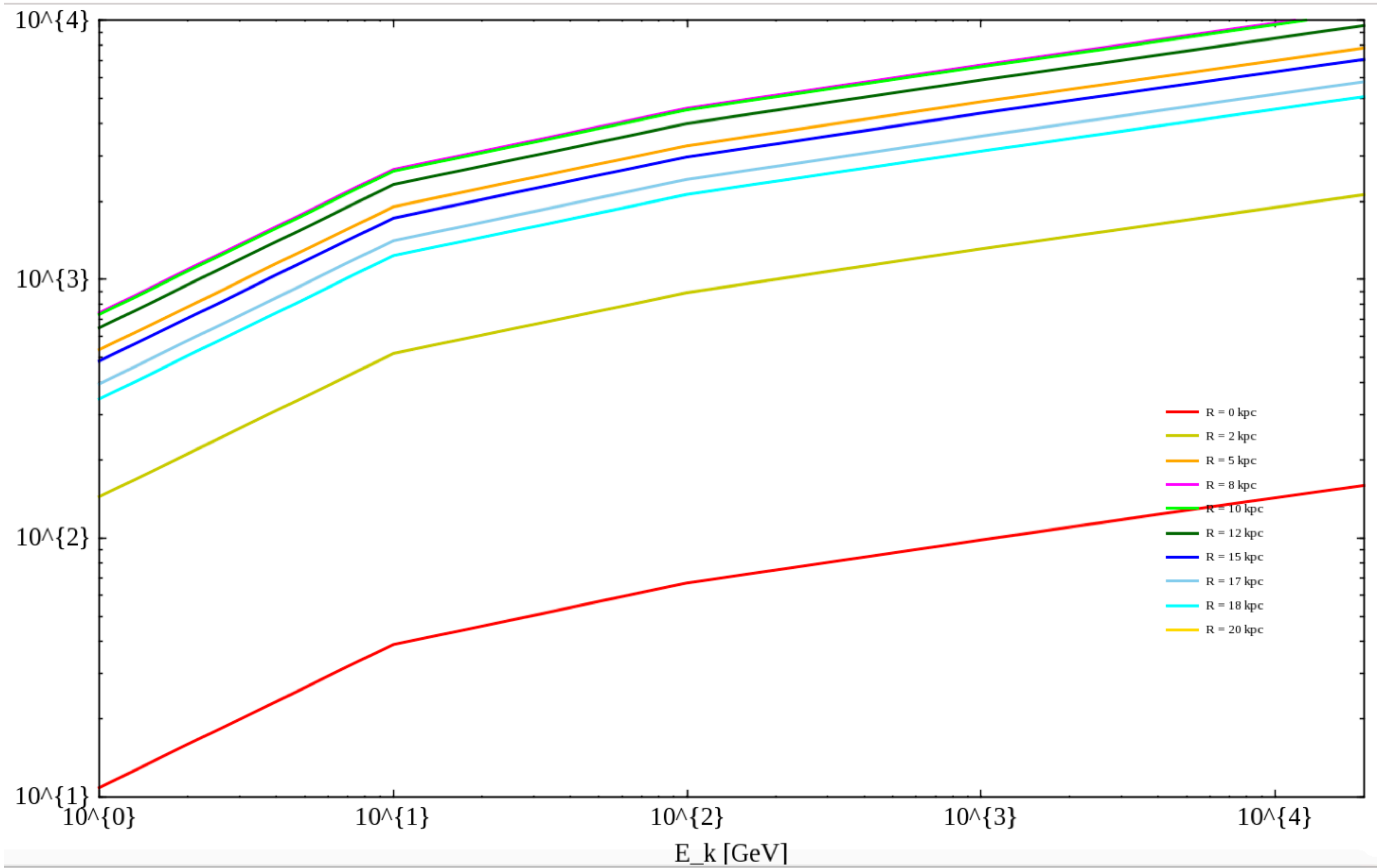

10^{4}
10^{3}
10^{2}
10^{1}
10^{0}
10^{1}
10^{2}
10^{3}
10^{4}
E_k [GeV]
R = 0 kpc
R = 2 kpc
R = 5 kpc
R = 8 kpc
R = 10 kpc
R = 12 kpc
R = 15 kpc
R = 17 kpc
R = 18 kpc
R = 20 kpc

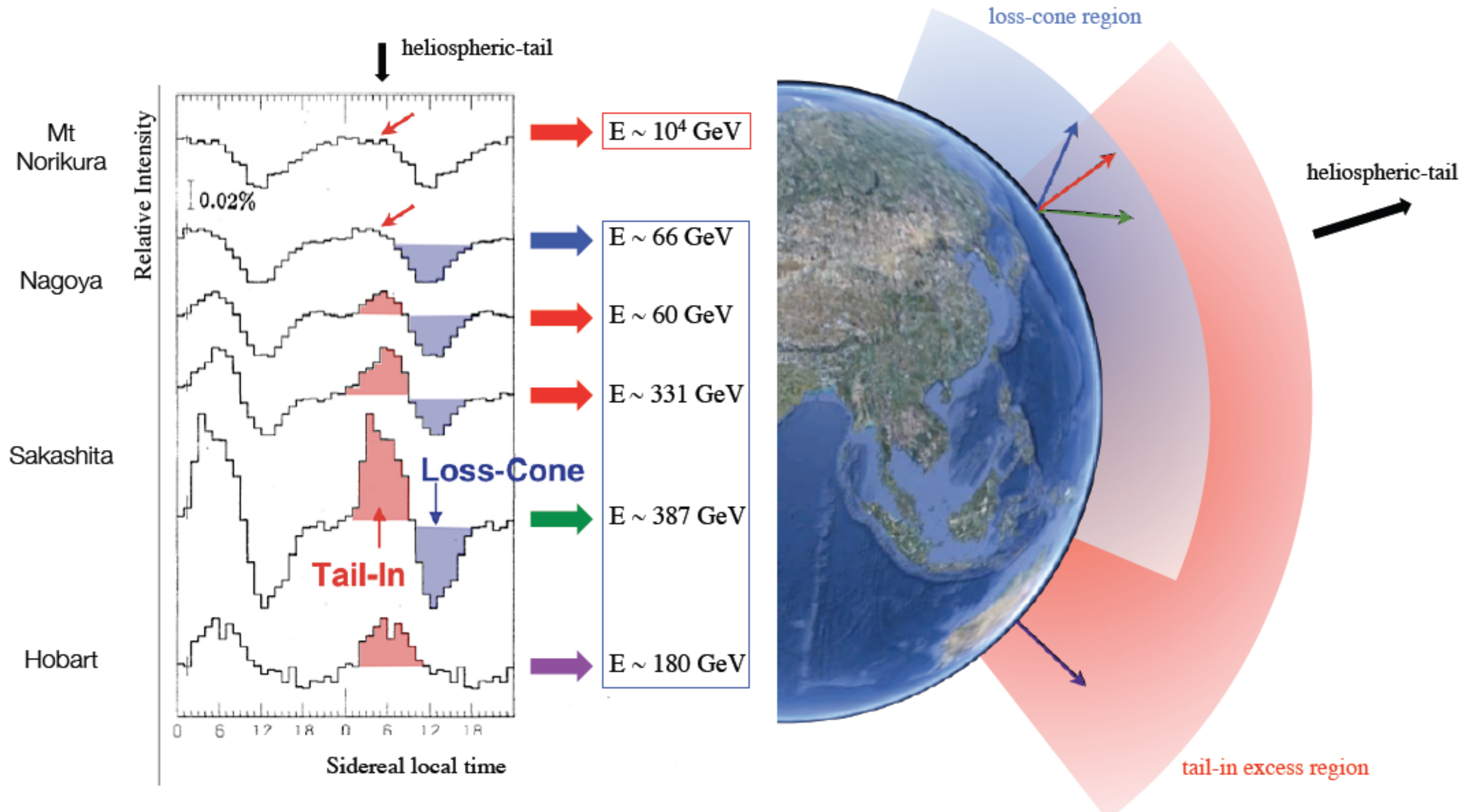

heliospheric-tail
Mt Norikura
Nagoya
Sakashita
Hobart
Relative Intensity
0.02%
Loss-Cone
Tail-In
Sidereal local time
0
6
12
18
0
6
12
18
E ~ 10^4 GeV
E ~ 66 GeV
E ~ 60 GeV
E ~ 331 GeV
E ~ 387 GeV
E ~ 180 GeV
loss-cone region
heliospheric-tail
tail-in excess region

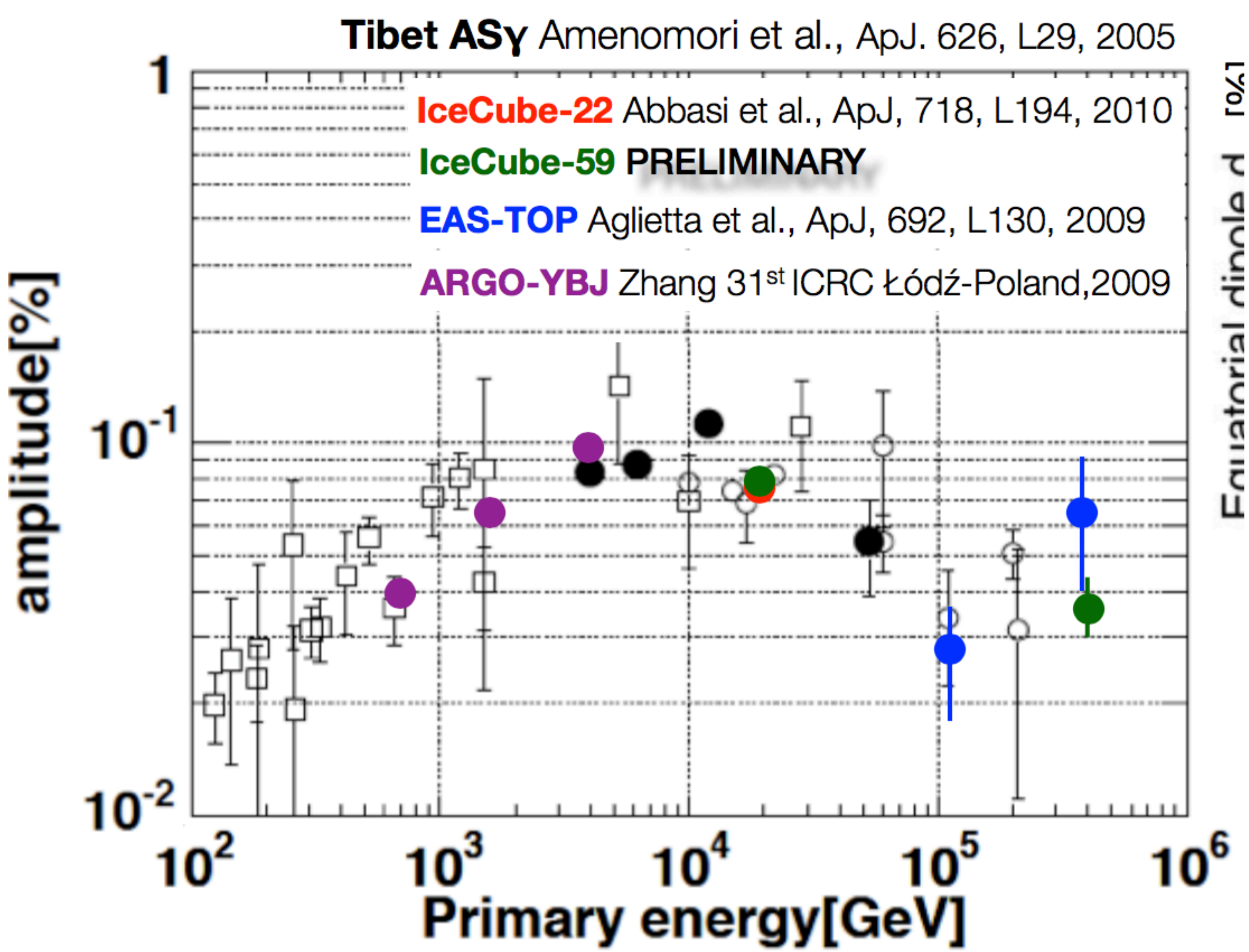

$3 \cdot 10^{-5}$ | $3 \cdot 10^{-4}$ | $3 \cdot 10^{-3}$ | $3 \cdot 10^{-2}$ | 0.3

7 | 70 | 700 | 7,000 | 70,000

heliospheric influence | galactic influence

$$B_\phi^{\rm disk}(R,z) \;=\; \begin{cases} B_{D0}\, e^{-|z|/z_0} & (R < R_{cD}) \\ B_{D0}\, e^{-|z|/z_0}\, e^{-(R-R_\odot)/R_0} & (R > R_{cD}) \end{cases} ,$$

$$B_\phi^{\rm halo}(R,z) \;=\; B_{H0}\left[1+\left(\frac{|z|-z_0^H}{z_1^H}\right)\right]^{-1} \frac{R}{R_O^H}\, e^{\left(1-\frac{R}{R_0^H}\right)}$$

$$B_z^{\rm pol}(R,z) \;=\; B_{\rm X}(R,z)\,\cos\left[\Theta_{\rm X}(R,z)\right],$$

$$B_R^{\rm pol}(R,z) \;=\; B_{\rm X}(R,z)\,\sin\left[\Theta_{\rm X}(R,z)\right],$$

$$B_{\rm X}(R,z) \;=\; \begin{cases} B_{\rm X}^0\,\left(\frac{R_p}{R}\right)^2 e^{-R_p/R_{\rm X}} & (R \le R_{\rm X}^c) \\ B_{\rm X}^0\,\left(\frac{R_p}{R}\right) e^{-R_p/R_{\rm X}} & (R > R_{\rm X}^c) \end{cases} ,$$

$$\Theta_{\rm X}(R,z) \;=\; \begin{cases} \tan^{-1}\left(\frac{|z|}{R-R_p}\right) & (R \le R_{\rm X}^c) \\ \Theta_{\rm X}^0 & (R > R_{\rm X}^c) \end{cases} ,$$

$$R_p \;=\; \begin{cases} \frac{R R_{\rm X}^c}{R_{\rm X}^c + |z|/\tan\Theta_{\rm X}^0} & (R \le R_{\rm X}^c) \\ R - \frac{|z|}{\tan\Theta_{\rm X}^0} & (R > R_{\rm X}^c) \end{cases} ,$$

$$\frac{\partial \psi}{\partial t} - \kappa \left[\frac{1}{r} \frac{\partial}{\partial r} \left(r \frac{\partial \psi}{\partial r} \right) + \frac{\partial^2 \psi}{\partial z^2} \right] = Q(r, z, E) \ ,$$

$$\rightarrow \frac{\partial \psi}{\partial t} - 2\kappa \frac{1}{r} \frac{\partial}{\partial r} \left(r \frac{\partial \psi}{\partial r} \right) - \kappa \frac{\partial^2 \psi}{\partial z^2} = Q'(r, z, E) \ ,$$

or

$$\rightarrow \frac{\partial \psi}{\partial t} - \kappa \frac{1}{r} \frac{\partial}{\partial r} \left(r \frac{\partial \psi}{\partial r} \right) - 2\kappa \frac{\partial^2 \psi}{\partial z^2} = Q'(r, z, E) \ ,$$

$$Q'(r, z, E) = Q(r, z, E) - \kappa \frac{1}{r} \frac{\partial}{\partial r} \left(r \frac{\partial \psi}{\partial r} \right) \ ,$$

or

$$Q'(r, z, E) = Q(r, z, E) - \kappa \frac{\partial^2 \psi}{\partial z^2} \ ,$$

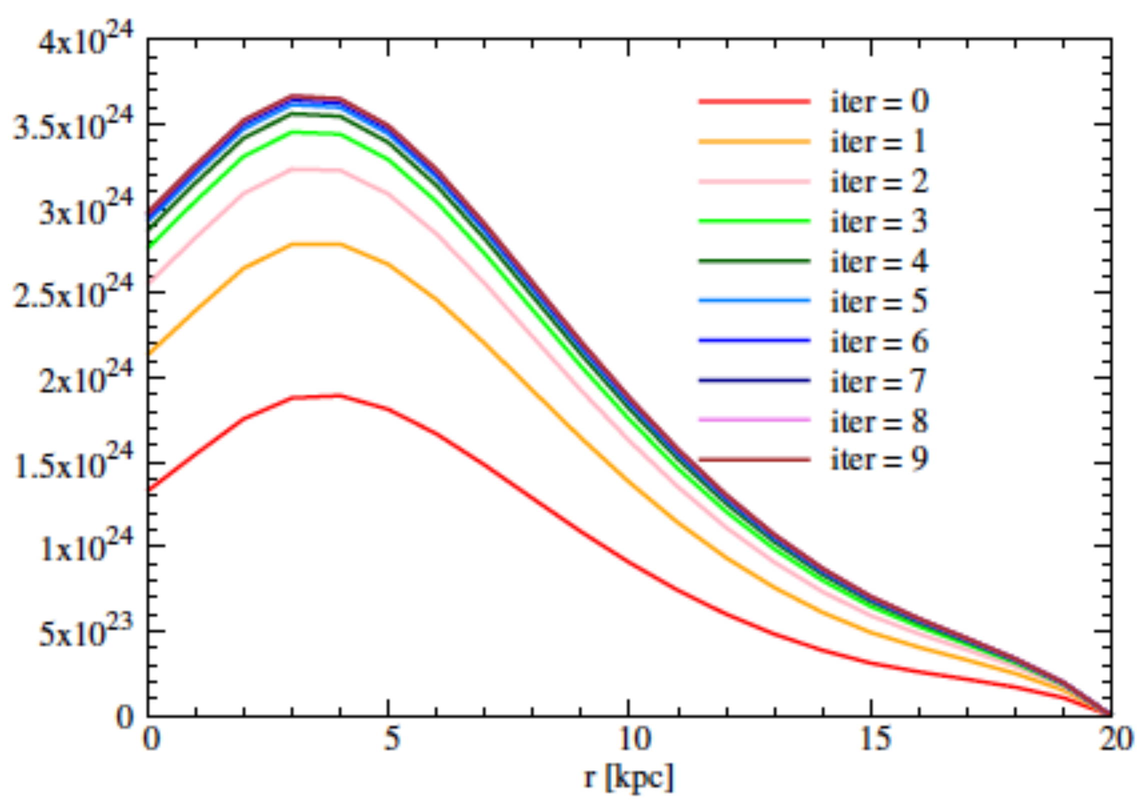

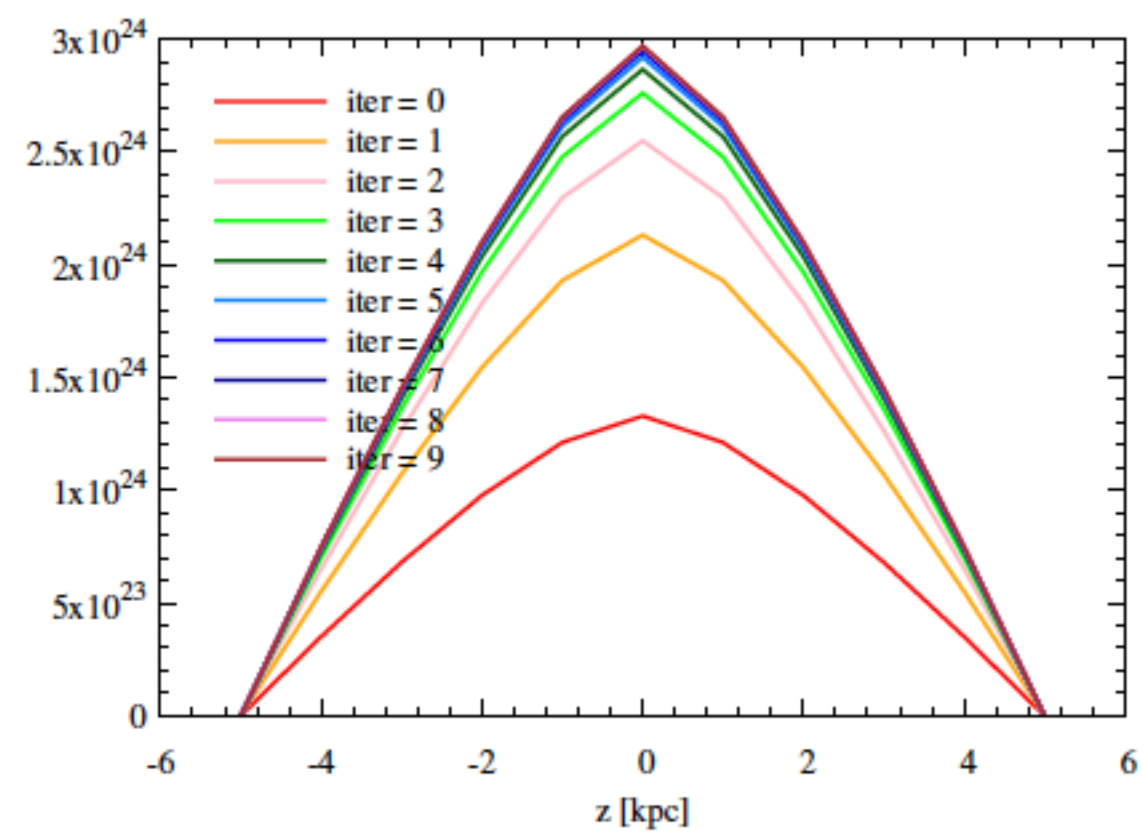

$$\kappa'_{\mu\nu} = \hat{R}_\theta \kappa_{\mu\nu} \hat{R}_\theta^{-1} \,,$$
$$= \begin{pmatrix} \cos\theta & \sin\theta & 0 \\ -\sin\theta & \cos\theta & 0 \\ 0 & 0 & 1 \end{pmatrix} \begin{pmatrix} D_{xx} & 0 & 0 \\ 0 & D_{yy} & 0 \\ 0 & 0 & D_{zz} \end{pmatrix} \begin{pmatrix} \cos\theta & -\sin\theta & 0 \\ \sin\theta & \cos\theta & 0 \\ 0 & 0 & 1 \end{pmatrix}$$
$$= \begin{pmatrix} D_{xx}\cos^2\theta + D_{yy}\sin^2\theta & (D_{yy}-D_{xx})\sin\theta\cos\theta & 0 \\ (D_{yy}-D_{xx})\sin\theta\cos\theta & D_{xx}\sin^2\theta + D_{yy}\cos^2\theta & 0 \\ 0 & 0 & D_{zz} \end{pmatrix}$$

$$\hat{R}_\theta = \begin{pmatrix} \cos\theta & \sin\theta & 0 \\ -\sin\theta & \cos\theta & 0 \\ 0 & 0 & 1 \end{pmatrix}$$

$$B_X(R,z) = \begin{cases} B_X^0 \left(\frac{R_p}{R}\right)^2 e^{-R_p/R_X} & (R \le R_X^c) \\ B_X^0 \left(\frac{R_p}{R}\right) e^{-R_p/R_X} & (R > R_X^c) \end{cases} ,$$

$$\Theta_X(R,z) = \begin{cases} \tan^{-1}\left(\frac{|z|}{R-R_p}\right) & (R \le R_X^c) \\ \Theta_X^0 & (R > R_X^c) \end{cases} ,$$

$$R_p = \begin{cases} \frac{R R_X^c}{R_X^c + |z|/\tan\Theta_X^0} & (R \le R_X^c) \\ R - \frac{|z|}{\tan\Theta_X^0} & (R > R_X^c) \end{cases} ,$$

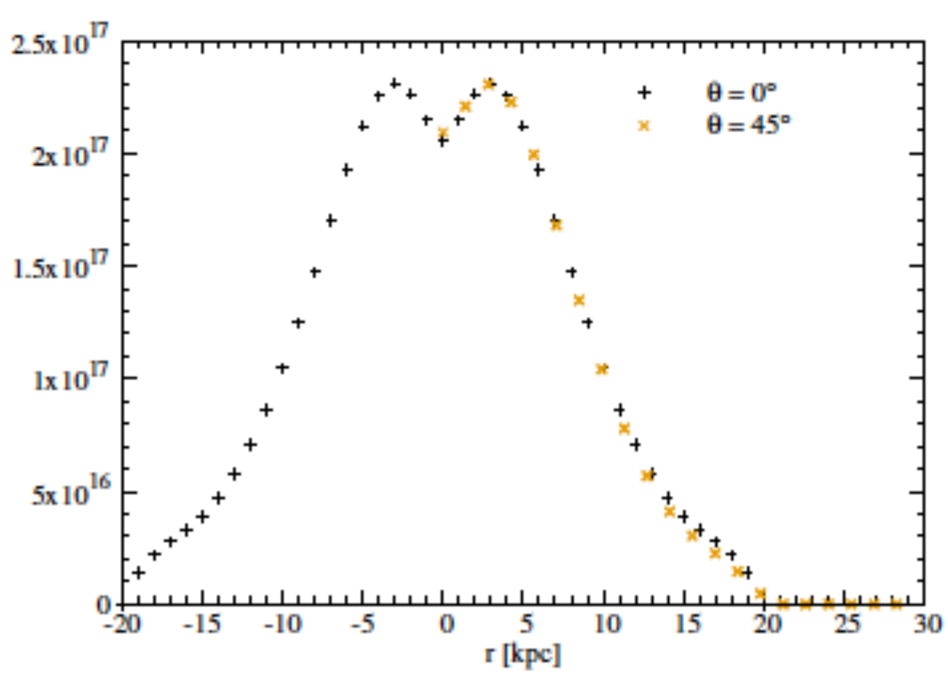

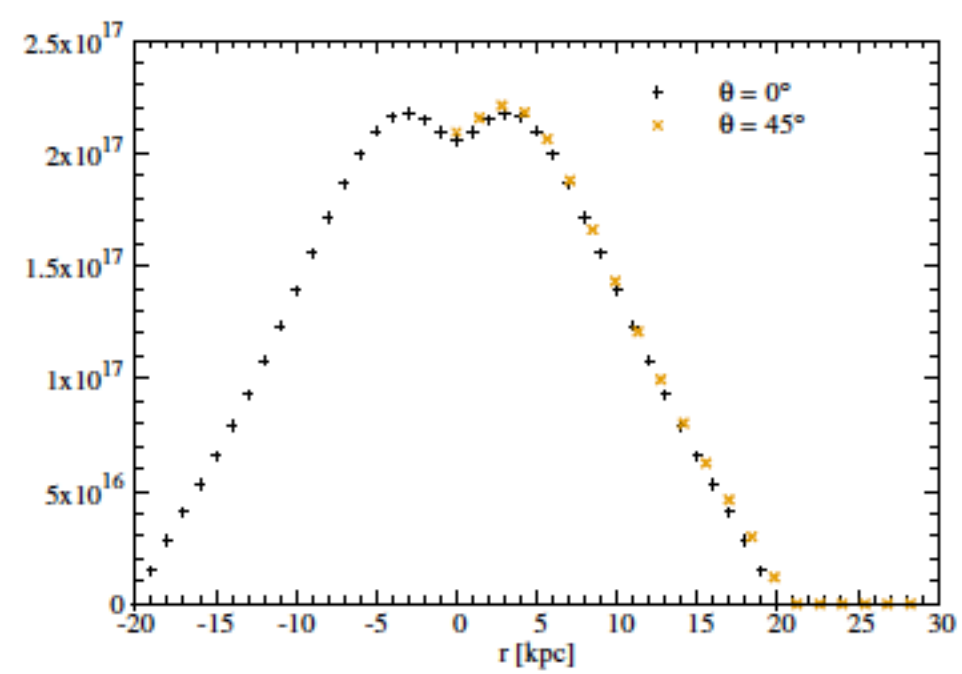

$$Q = -\nabla\cdot(D\cdot\nabla)\psi = -\left(\frac{\partial^2\psi}{\partial x^2}+\frac{\partial^2\psi}{\partial y^2}+\frac{\partial^2\psi}{\partial z^2}+2\frac{\partial^2\psi}{\partial x\partial y}\right)$$
$$=({k_x}^2 D_{xx}+{k_y}^2 D_{yy}+{k_z}^2 D_{zz})\cos k_x x\cos k_y y\cos k_z z$$
$$-2k_x k_y D_{xy}\sin k_x x\sin k_y y\cos k_z z$$

$$Q' = Q + S, S = 2\frac{\partial^2\psi'}{\partial x\partial y}$$

$$\begin{pmatrix} D_{xx}\cos^2\theta + D_{yy}\sin^2\theta & (D_{yy}-D_{xx})\sin\theta\cos\theta & 0 \\ (D_{yy}-D_{xx})\sin\theta\cos\theta & D_{xx}\sin^2\theta + D_{yy}\cos^2\theta & 0 \\ 0 & 0 & D_{zz} \end{pmatrix}$$

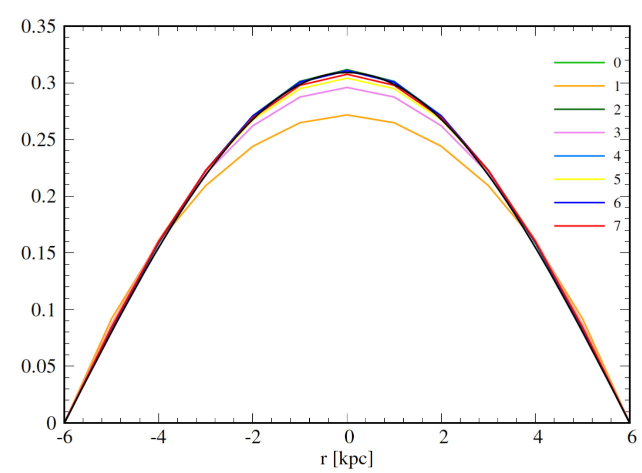

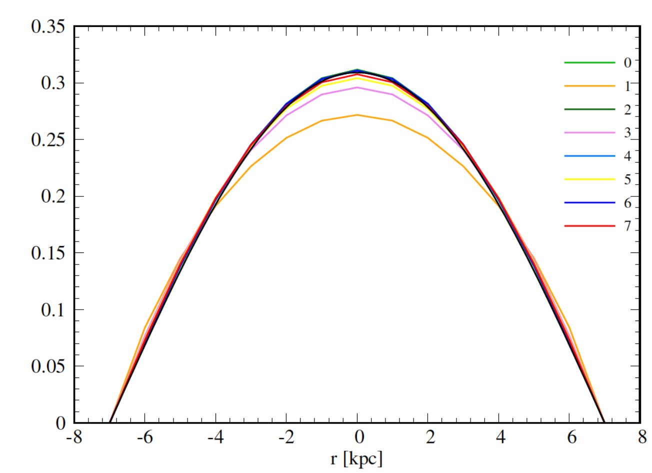

$$\kappa'_{\mu\nu} = \begin{pmatrix} \frac{(D_{xx}+D_{yy})}{2} & \frac{(D_{yy}-D_{xx})}{2} & 0 \\ \frac{(D_{yy}-D_{xx})}{2} & \frac{(D_{xx}+D_{yy})}{2} & 0 \\ 0 & 0 & D_{zz} \end{pmatrix}$$

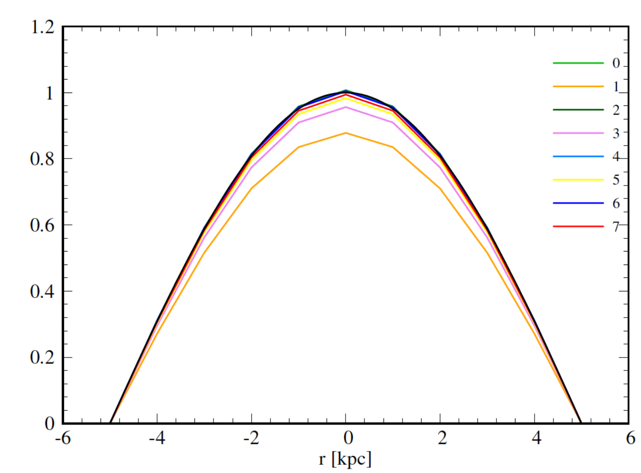

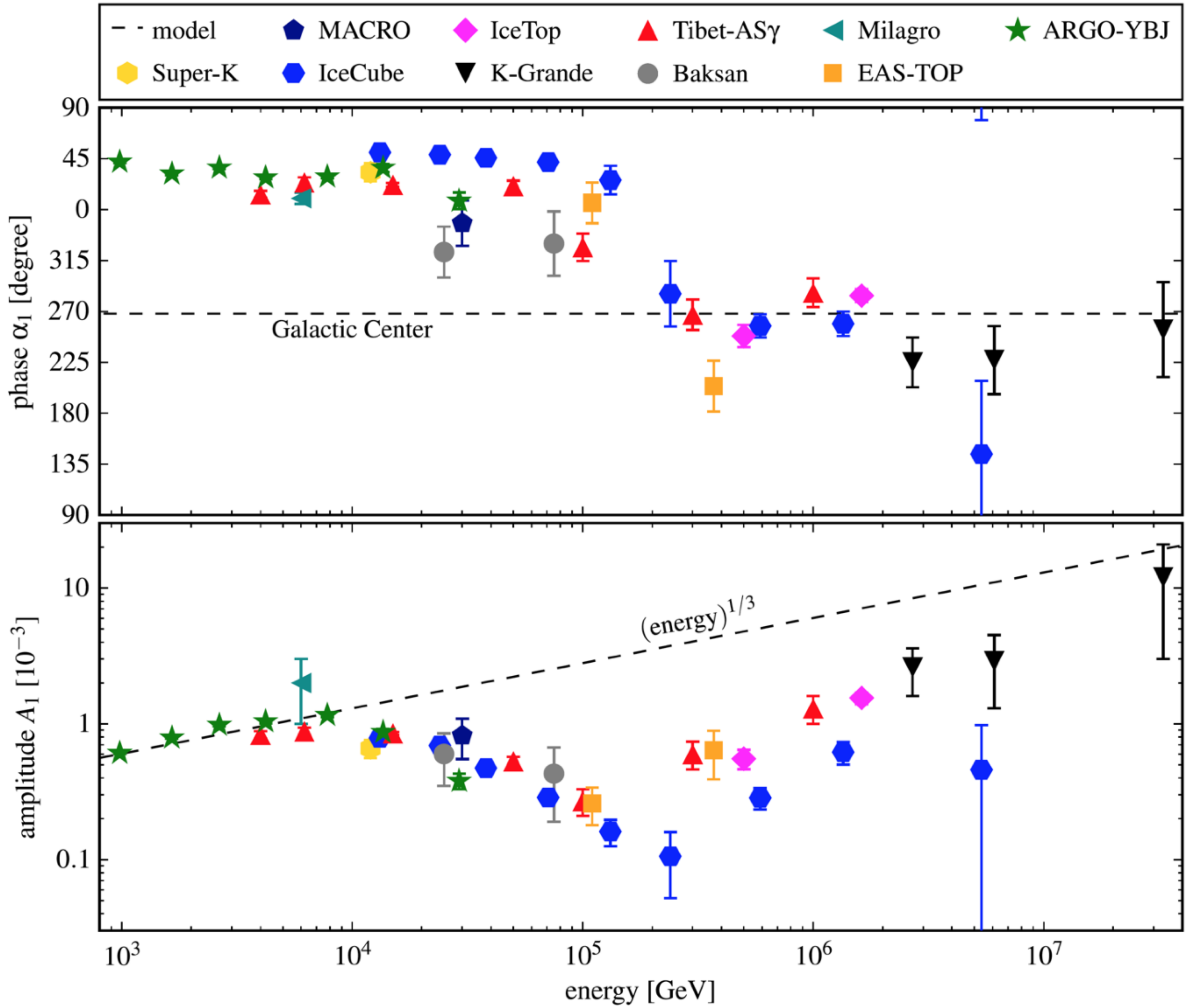

10^{12}

10^{13}

10^{14}

10^{15} 10^{16}

Phase and amplitude of the (equatorial) dipole anisotropy, from 2017PrPNP.. 94..184A

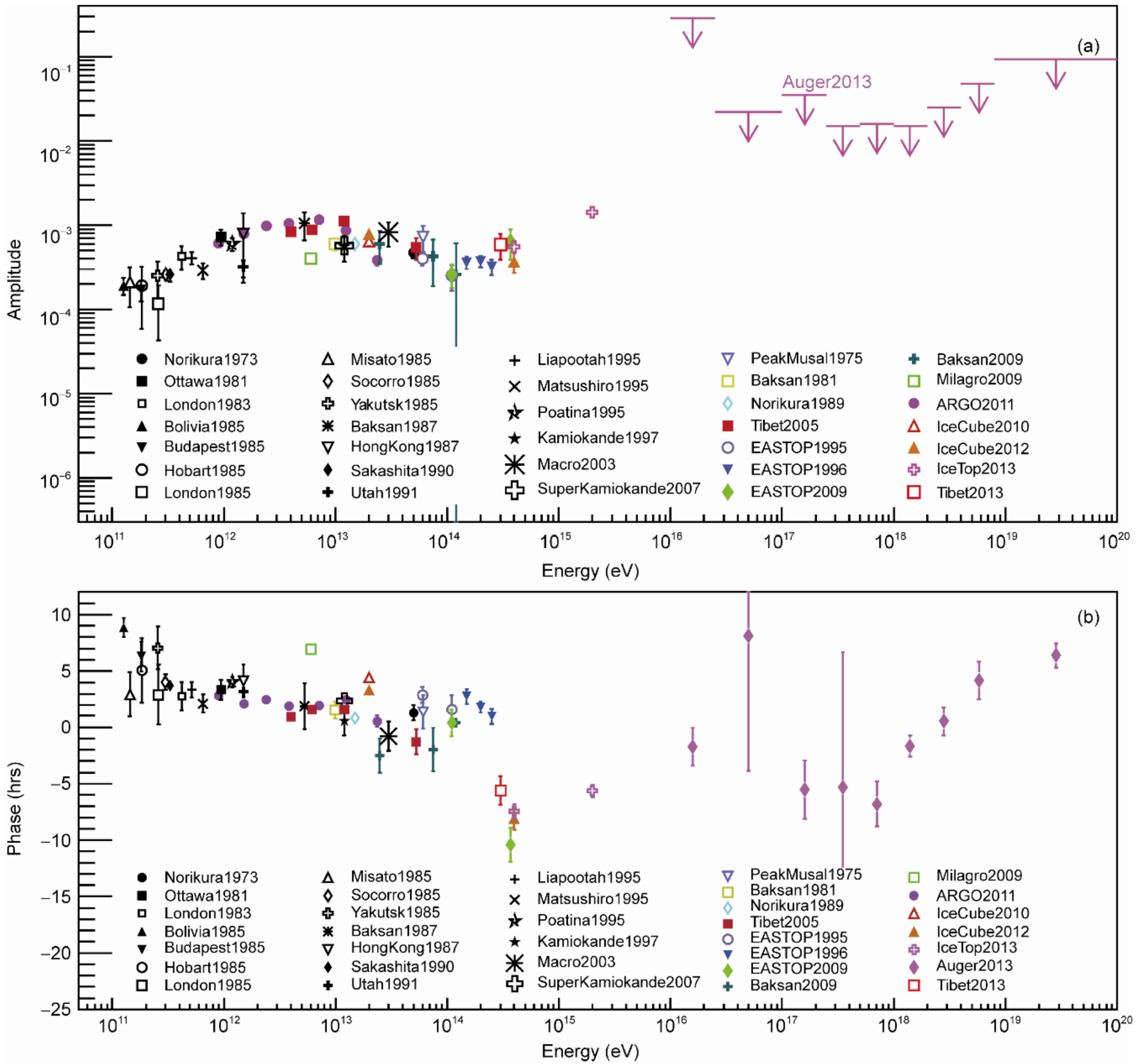

Phase and amplitude of the (equatorial) dipole anisotropy, H. B. Hu and Y. Q. Guo 2016

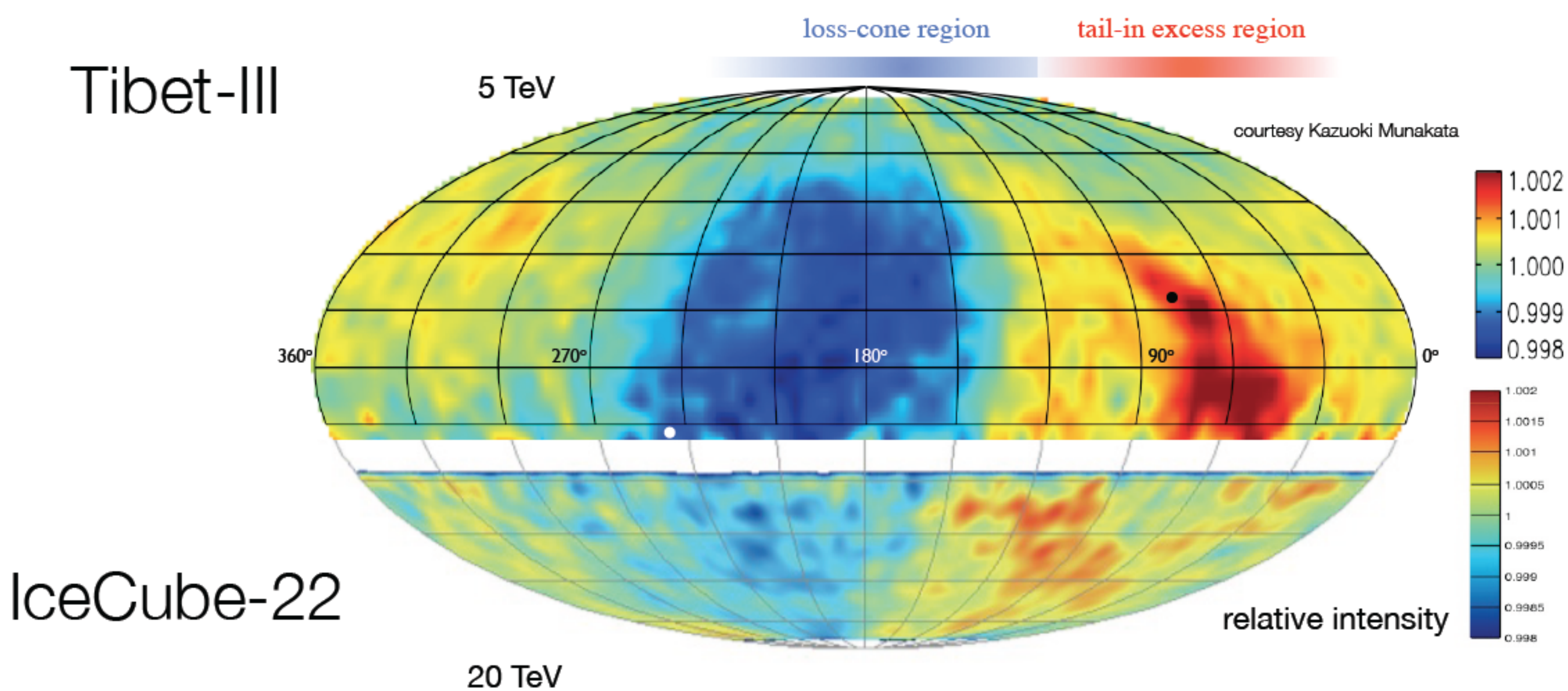
Tibet-III
5 TeV
loss-cone region
tail-in excess region
courtesy Kazuoki Munakata
360°
270°
180°
90°
0°
1.002
1.001
1.000
0.999
0.998
1.002
1.0015
1.001
1.0005
1
0.9995
0.999
0.9985
0.998
relative intensity
IceCube-22
20 TeV

Spatial-dependent diffusion

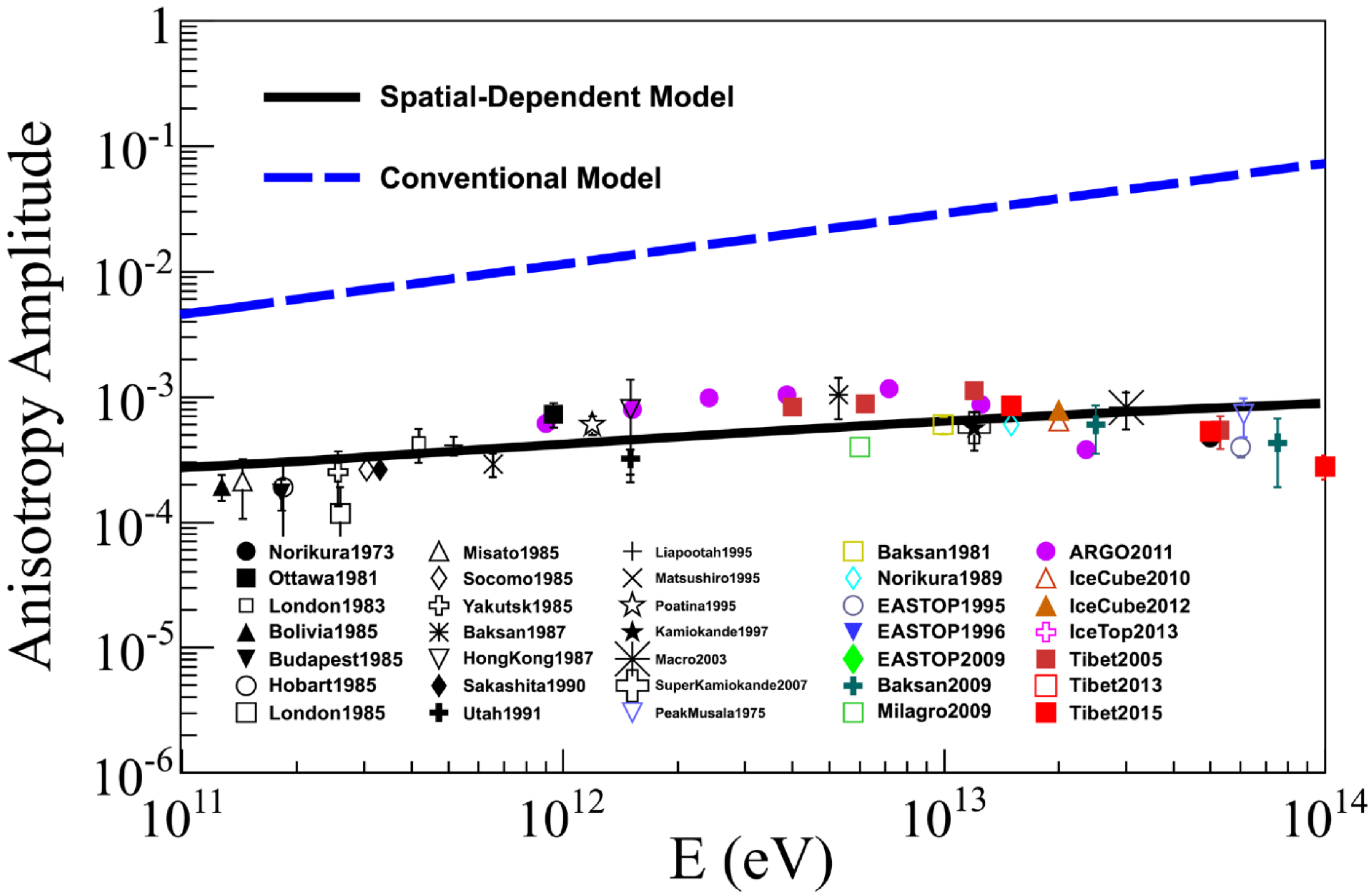

Y. Q. Guo, Z. Tian, and C. Jin, 2016ApJ…819...54G

Nearby source

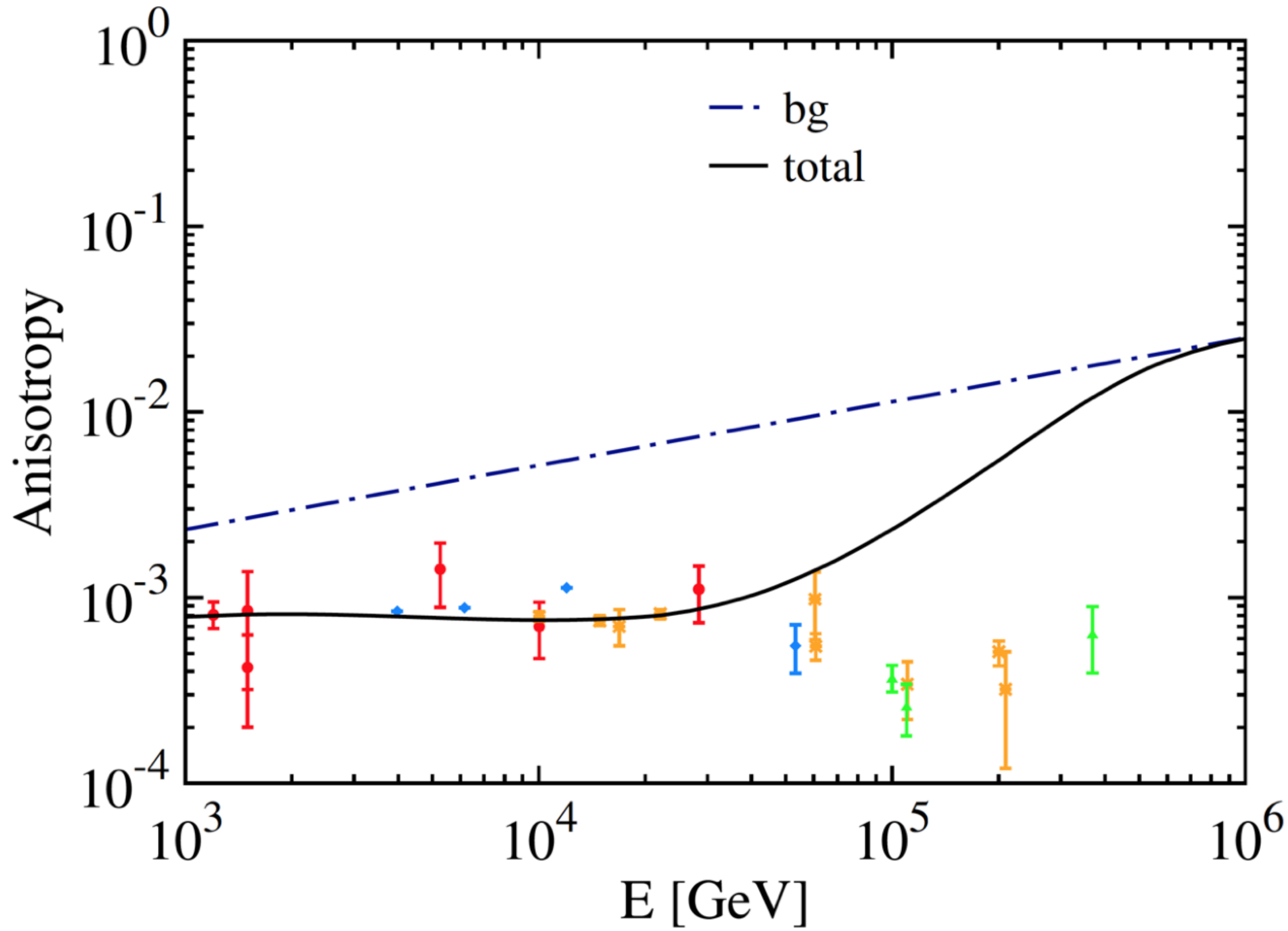

W. Liu, X. J. Bi, S. J. Lin, B. B. Wang, and P. F. Yin, 2017PhRvD..96b3006L

P. Blasi, E. Amato, 2012JCAP…01..011B

Ordered magnetic fields are also observed out to large distances from the plane, i.e. radio halos, with X-shaped patterns.

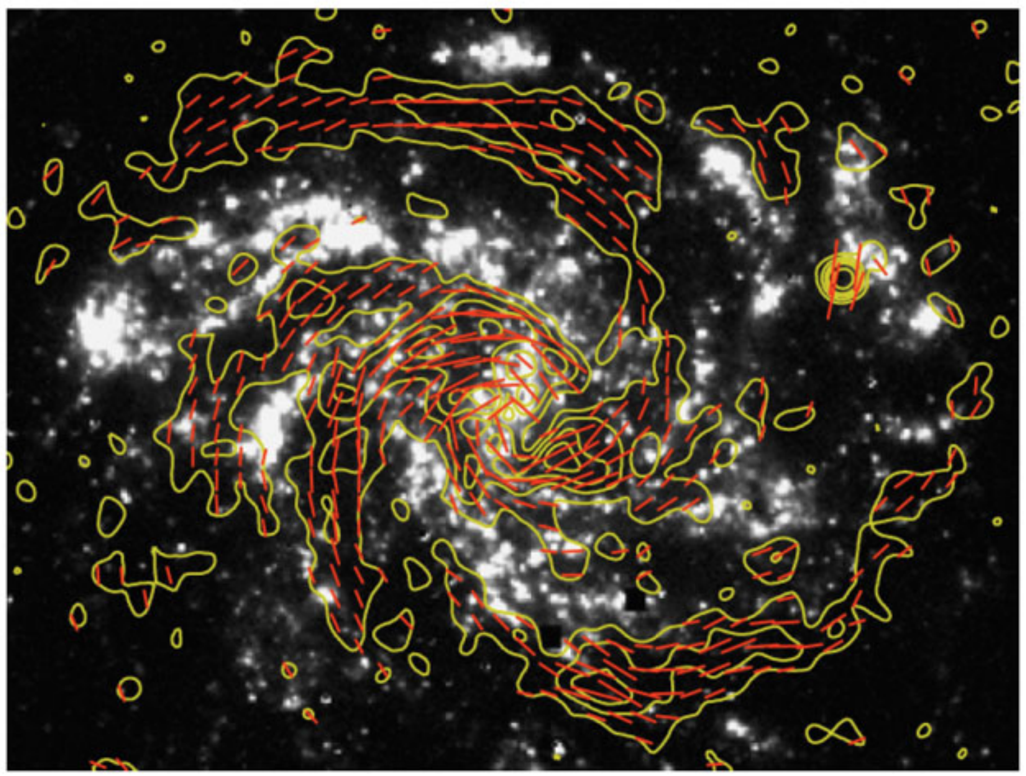

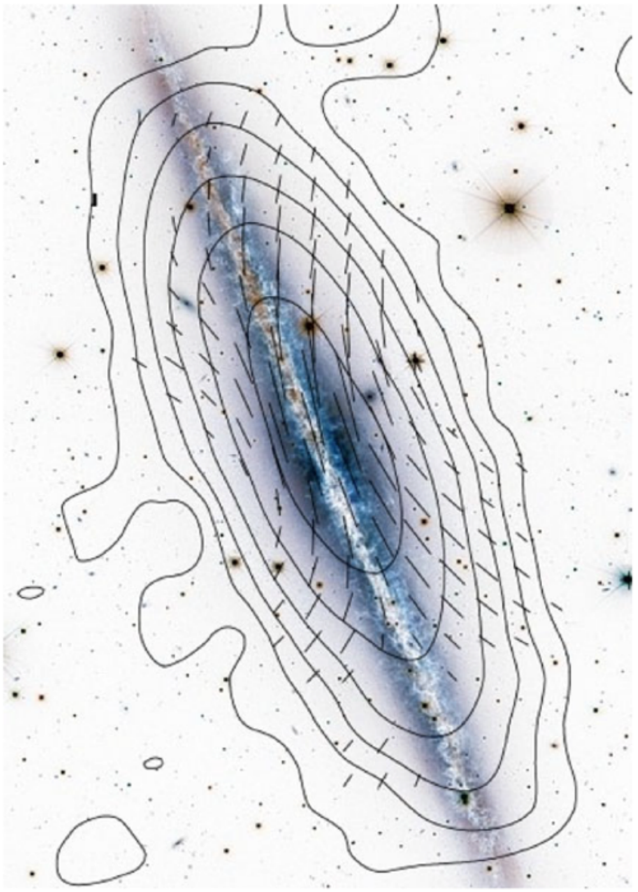

The radio continuum observations of nearby spiral galaxies infer .